Identification of transcriptomic responses related to normal, healthy and accelerated aging

César Payán Gómez

Director

Prof. Sandra Ramírez-Clavijo, PhD

Universidad del Rosario

Universidad del Rosario

Faculty of Natural Sciences and Mathematics

School of Medicine and Health Sciences

Doctorate in Biomedical Sciences

2018

CONTENTS

LIST OF TABLES

page

Chapter 1

Chapter 2

LIST OF TABLES

Page

Chapter 3

LIST OF FIGURES

LIST OF ABBREVIATIONS

CNS	central nervous system
CR	calorie restriction
CS	Cockayne syndrome
DA	dopaminergic
DEG	Differentially expressed gene
DR	Dietary restriction
FC	fold change
GG-NER	global genome repair
ILBD	incidental Lewy body
IPA	Interactive pathway analysis
IRI	Ischemia-reperfusion injury
ND	neurodegenerative diseases
ORA	overrepresentation analysis
PCA	Principal component analysis
PD	Parkinson´s disease
PFC	prefrontal cortex
QC	quality control
TCR-NER	transcription-coupled nucleotide excision repair
TF	transcription factor
TO	target of rapamycin
TTD	trichothiodystrophy
XP	xeroderma pigmentosum

SUMMARY

Aging is defined as the reduction in the physiological and adaptive capabilities of organisms with the passage of time. There is increased susceptibility to cardiovascular and neurodegenerative diseases, cancer and diabetes, among others (1). Aging is a complex biological process which occurs in almost all organisms and is associated with a progressively diminishing capacity for homeostasis and physiological functions.

The causes associated with the appearance of aging are not fully known. Multiple lines of evidence suggest that the accumulation of DNA damage could be the central event on which other factors related to the aging process coalesce (2). One of the links most clearly connecting DNA damage to aging are the progeroid syndromes caused by a deficiency of DNA transcription-coupled nucleotide excision repair (TCR-NER) subpathway (3). TCR-NER is activated in response to RNA polymerase II-blocking during transcription.

Surprisingly, there is a parallel between the transcriptional response of progeroid mice and mice on a dietary restriction (DR) regimen (an intervention that extend the lifespan). DR even for short periods of time, has increased resistance to different forms of acute stress (4) such as ischemia-reperfusion injury, a characteristic lesion of transplants or vaso-occlusive disease (5). Corroborating that TCR-NER deficiency induces activation of similar protective mechanisms, Csb-/- and Csa-/- mice are less susceptible to renal ischemia-reperfusion injury (6).

The parallel between the transcriptomic and metabolic responses of animals at two life expectancy extremes, in addition to the shared increase in resistance to ischemia-reperfusion injury, has been explained by the existence of a programmed survival response. This response would be activated by low-intensity stress, promoting the mobilization of the organism´s resources towards protection and inhibiting growth-related processes (7). The survival response has not been completely characterized; its activation or protection mechanisms are not clearly known, nor what type of interventions would prompt it, how the response would vary with respect to the organism´s lifespan, and whether or not different types of low-intensity stress would produce greater activation.

This thesis addresses several questions related with the survival response, the mechanism of neurodegeneration and normal aging using mainly analysis of transcriptomic data.

First, it was established that old mice are able to activate an incomplete survival response after three days of DR, second, a common mechanism of activation of the protective response was described. Third, a connection between the accumulation of DNA damage and neurodegeneration was provided. Finally to have a complete vision of the process of aging, an integrative methodology of analysis was used over brain human transcriptomic data, the result was the identification of an opposite activation of astrocytes in the human aged prefrontal cortex.

1. GENERAL INTRODUCTION

Aging is defined as the reduction in the physiological and adaptive capabilities of organisms with the passage of time. There is increased susceptibility to cardiovascular and neurodegenerative diseases, cancer and diabetes, among others (1). With the progressive aging of the population due to decreased birth rates and increased life expectancy, it has become one of the most important public health problems (8). Therefore, healthcare systems must include programs to improve the quality of life of this sector of the population, and these programs must address prevention, early diagnosis of several diseases and treatment of chronic diseases, with the resulting increase in healthcare system costs.

One of the challenges of today´s medicine is understanding the molecular mechanisms of aging in order to be able to identify biomarkers of biological age, the diagnostic predictors and state of typical aging-associated diseases, and, finally, strategies for modulating the aging process.

Aging is a complex biological process which occurs in almost all organisms and is associated with a progressive diminishing capacity for homeostasis and physiological functions. It is characterized by a progressive accumulation of damage in various cellular and subcellular systems. On the cellular level, there is an accumulation of senescent cells, a decrease in stem cells, a decreased capacity to respond to injury, changes in morphology and functional deterioration. The disrupted subcellular processes include telomere shortening, epigenetic modifications, loss of proteostasis, mitochondrial dysfunction, poor cellular communication and genomic instability (9).

The causes associated with the appearance of aging are not fully known. However, there are various theories that explain the development of some of the previously mentioned disruptions.

The most widely accepted hypotheses are:

Crosslinking/glycation: With age, macromolecules such as DNA and proteins form cross linkages with each other and with glucose. These cross linkages decrease molecular function and elasticity, and also inhibit protease activity. Therefore, these damaged molecules accumulate in the tissues and cause characteristic aging problems such as cardiomegaly and brain function deterioration (10).

Oxidative damage: The free radicals which escape from the neutralization systems may damage DNA, proteins, lipids and mitochondria. This type of damage is known as oxidative damage and causes accumulation of abnormal molecules which disrupt the synthesis of DNA, RNA and proteins. In addition, it interferes with cellular communication and energy production, generally altering normal cell function (11).

Replicative senescence: Cellular senescence consists of cessation of cellular division. Cells have a limited capacity for reproduction through mitosis; each time a cell divides, it loses a small part of its telomeres. When the telomeres reach a critical level of shortening, the cell cannot replicate its genome any more, and stops dividing. The activation of oncogenes, oxidative stress and DNA damage also induce cellular senescence. This process has been associated with aging-associated diseases such as fatty liver, diabetes and tumor genesis (12).

Accumulation of DNA damage: DNA is susceptible to injury due to various factors such as oxidative stress, replication errors, toxins or radiation. Most of the damage is eliminated by the DNA repair systems; the fraction of the damage that is not repaired accumulates, and may eventually cause the cells to malfunction (2).

Multiple lines of evidence suggest that the accumulation of DNA damage could be the central event on which other factors related to the aging process coalesce (2). One of the links most clearly connecting DNA damage to aging is the progeroid syndromes. These are monogenic diseases characterized by premature aging and may or may not be associated with an increased incidence of cancer. The connection between the accumulation of DNA damage and aging lies in the fact that one group of these progeroid syndromes is caused by a mutation in the genes which code for proteins from the DNA transcription-coupled nucleotide excision repair (TCR-NER) subpathway (3).

The NER pathway is activated in response to a wide range of types of damage which cause a distortion in the helical DNA structure. This repair mechanism is divided in two subpathways: global genome repair (GG-NER) and transcription-coupled repair (TCR-NER). These subpathways differ in their initial DNA damage recognition mechanisms. GG-NER recognizes damage anywhere in the genome through the protein dimer XPC-hHR23B (13). TCR-NER is activated in response to RNA polymerase II blocking during transcription; therefore, it identifies damage in transcriptionally active genes. The CSB and CSA proteins are responsible for identifying this damage. The next steps in DNA damage repair are similar for both subpathways. The transcription factor TFIIH, which contains two helicases with opposite polarities (XPB and XPD), is recruited in the damaged region, along with the XPG endonuclease. These proteins unroll the DNA around the injury. Subsequently, the XPA protein attaches to the lesion site, probably to allow other repair proteins to be recruited and to ensure that the damage is correctly eliminated. Then, the endonuclease dimer ERCC1/XPF cuts the region flanking the damage, the damaged section is removed, and the resulting gap is filled by template-dependent polymerization (14).

In humans and mouse models with GG-NER deficiency, such as occurs in xeroderma pigmentosum (XP), the inability to repair DNA damage is related to a greater predisposition to cancer. Meanwhile, in TCR-NER repair subpathway defects, such as trichothiodystrophy (TTD), Cockayne syndrome (CS) and XFE progeroid syndrome, there is a dominant phenotype of premature aging without a predisposition to cancer (2). This collection of syndromes evidences the existence of a connection between the accumulation of DNA damage and aging.

Knockout mice with mutations identified in humans with these diseases have been characterized with regard to the progeroid phenotype. Several studies have found that mouse models recreate normal aging very accurately, except at a greater speed. The TTD mouse, with an Xpd gene mutation similar to that found in a TTD patient, develops bone fragility and premature loss of stem cells (15). Cockayne syndrome group A (Csa -/-) and Cockayne syndrome group B (Csb m/m) mutant mice have a greater sensitivity to UV radiation, accelerated loss of photoreceptors, decreased body weight and moderate neurological abnormalities (16, 17), similar to a moderate CS phenotype in humans. Mice with double mutations in CSB and XPA (Csbm/m;Xpa-/-) develop a more severe phenotype, with decreased postnatal growth, progressive kyphosis, ataxia, retinal degeneration, motor dysfunction and premature death (18). Mice with loss of Ercc1 (Ercc1-/-) expression have a phenotype very similar to that of people with XFE syndrome, with pre and postnatal growth retardation, skin,

liver and bone marrow abnormalities, and a life expectancy of only four weeks (19). The compound homozygous Ercc1 -/Δ mouse with a null mutation in one Ercc1 allele and a deletion causing the loss of seven amino acids on the carboxyl terminal end of the other allele, has a less severe phenotype compared to that of Ercc1-/-. This phenotype is characterized by accelerated hearing and vision loss, motor neuron degeneration, liver and kidney abnormalities with cytoplasmic invaginations and polyploid cells, lack of subcutaneous fat and a decreased life expectancy (20-22).

The combination of these results leads to the conclusion that the typical progeroid phenotype of this type of syndromes is related to the decreased capacity to repair DNA damage in transcriptionally active genes. In addition, the fact that the most severe phenotypes are related to greater TCR-NER deficiencies indicates that the accumulation of mutations is responsible for progeria. This evidence is compatible with the possibility of natural aging being caused by the slow and progressive accumulation of DNA mutations, mainly those that affect transcriptionally active genes.

Transcriptomics is very useful for studying complex phenotypes such as normal aging and progeria, since it allows the identification of molecular processes associated with the trait of interest through hypothesis-free studies. A comparison of the liver transcriptome of TCR-NER deficient mice and that of wild mice with natural aging shows important parallels. The liver transcriptome of 15 day old Csbm/m;Xpa-/- and Ercc1-/- mice and 16 week old Ercc1-/ Δ mice along with aged 96 and 130 week old wild mice shows suppression of the genes for oxidative metabolism, cellular growth and energy reserve homeostasis (7, 18, 19).

These same analyses also showed that, in mice with a progeroid phenotype, the suppression of growth hormone/insulin-like growth factor 1 (GH/IGF-1) pathway genes leads to systemic suppression of the somatotropic axis. There is also an increased antioxidant response (7, 19, 23). Surprisingly, these changes are similar to those found in mice that have an increased life expectancy due to either dietary restriction (DR) or specific genotypes which suppress the GH/IGF-1 pathway (7). The proposed explanation of this parallel between two extremes of longevity is that both groups are exposed to continuous levels of stress, and they increase their somatic protection mechanisms in response. In progeroid mice, the activator of these mechanisms would be genotoxic stress, while in mice subjected to DR the stressor would be the scant availability of food.

Mice on a DR regimen, even for short periods of time, have increased resistance to different forms of acute stress (4) such as ischemia-reperfusion injury, a characteristic lesion of transplants or vaso-occlusive disease (5). This protection is correlated with improved sensitivity to insulin, increased expression of genes related to the antioxidant response and decreased expression of inflammatory and IGF-1 signaling markers. Corroborating that TCR-NER deficiency induces activation of similar protective mechanisms, Csb-/- and Csa-/- mice are less susceptible to renal ischemia-reperfusion injury (6).

The parallel between the transcriptomic and metabolic responses of animals at two life expectancy extremes, in addition to the shared increase in resistance to ischemia-reperfusion injury has been explained by the existence of a programmed survival response. This response would be activated by low intensity stress, promoting the mobilization of the organism´s resources towards protection and inhibiting growth-related processes (7). The survival response has not been completely characterized; its activation or protection mechanisms are

not clearly known, nor what type of interventions would prompt it, how the response would vary with respect to the organism´s time of life, and whether or not different types of low intensity stress would produce greater activation.

The first part of this thesis addresses several of these questions through transcriptomics (chapter 1). Wild mice from different age groups subjected to various types of diet restriction were used as study models. The level of protection conferred on each of the experimental groups was determined, and finally, the transcriptomic response was characterized in order to identify molecular mechanisms associated with a greater resistance to stress.

On another note, the central nervous system (CNS) is significantly affected by the aging process; signs of this are the normal cognitive deterioration associated with age and the greater incidence in elderly people of neurodegenerative diseases (ND) such as Alzheimer´s and Parkinson´s disease. Thus, it is not surprising that both people with progeroid syndromes due to TCR-NER deficiency as well as mouse models with these syndromes should have phenotypes related to the premature loss of CNS function.

Traditionally, the consequences of defects in DNA damage repair have been studied in proliferating cells, and therefore the function of DNA repair in nervous tissue is relatively poorly understood (24). Reports on this subject mainly show associations between DNA damage and neurodegeneration. The role of the accumulation of DNA damage, and whether or not it is a definitive cause of neural dysfunction or death, is unknown (25). Due to the fact that homozygous mutations in TCR-NER genes produce a very severe phenotype, it is difficult to differentiate whether the CNS involvement depends directly on the accumulation of damage or if it is caused by systemic disruptions (26). In response to this, conditional mice which express the mutation in specific regions of the CNS have been studied. This type of studies has evidenced that rats with Ercc1-/Δ mutations restricted to the frontal cortex present age-dependent decreased neuronal plasticity and progressive neuronal disease compatible with a neurodegenerative process (27). These results confirm the importance of TCR-NER in normal CNS functioning. An implicit limitation in this type of model is that the accumulation of DNA damage occurs in an accelerated fashion, contrary to what is hypothesized for neurodegenerative diseases where decades of slow, progressive DNA damage accumulation are needed for the phenotype to be expressed. Likewise, at least in the initial stages of the diseases, the neuronal damage is confined to distinctive brain areas, and even to specific types of neurons (28-30). It is therefore necessary to investigate if the susceptibility of different encephalic zones may be related to TCR-NER levels, and if a slower, more progressive accumulation of DNA damage may also trigger neurodegenerative diseases.

Chapter 2 of this thesis studies these questions from a gene expression perspective. Parkinson´s disease (PD) was used as a neurodegenerative disorder model, and micro arrays and next-generation sequencing were used as transcriptomic tools. First, the levels of TCR-NER gene expression were explored in different brain regions of healthy people. Then, the *substantia nigra* of mice with marginal TCR-NER deficiency was characterized on the molecular level in order to make a parallel between the animal model and individuals with PD.

Finally, to have a complete vision of the process of aging, it is necessary to study it under normal conditions. Once again, transcriptomics is an ideal tool for this, as it identifies in a non-biased way which processes are the most relevant in the presentation of the phenotype of interest. However, this approach is not without limitations, such as the difficulty in obtaining

biological samples, if what is being studied is CNS aging in humans. One solution for this is to combine several small studies, thereby increasing statistical power and obtaining more robust lists of differentially expressed genes. The meta-analysis methods work very well for this purpose. Thus, the conclusion of this thesis consisted in combining several independent studies which identify levels of expression in the prefrontal cortex (PFC) of people from different age groups. The prefrontal cortex was chosen since it is one of the brain regions most susceptible to changes in the aging process.

Chapter 3 of this thesis reports the results of the combination of four studies on human PFC transcriptomic, emphasizing the role of astrocytes in successful aging.

1.2 OBJECTIVES

1.2.1 GENERAL

To identify transcriptomic responses related to normal, healthy and accelerated aging

1.2.2 SPECIFIC

To describe the transcriptomic response of aged mice to fasting as a model of protection against acute stress

To identify common pathways activated by different dietary and protective interventions against acute stress

To evaluate parallels and divergences among a model of mild deficient in TC-NER with molecular signatures of Parkinson´s disease

To describe the transcriptomic modifications in aged human prefrontal cortex

2. Chapter 1

Transcriptomic characterization of the protective survival response to high intensity acute stress

2.1 Introduction

Dietary restriction (DR) entails reducing the ingestion of a particular nutrient, without causing malnutrition. Dietary restriction protocols with regard to calorie ingestion, known as calorie restriction (CR), reduce dietary calories by 20-40%. With these levels of restriction, an extended life expectancy and a decreased appearance of age-related chronic diseases can be seen in a wide variety of species such as yeast, *Drosophila*, *C. elegans*, fish, mice, rats and primates (31). Although the mechanisms by which DR has a positive effect on longevity are not completely understood, there are several known pathways which are modulated by the nutritional intervention (32). Experimental models subjected to DR have modifications in the pathways regulated by the target of rapamycin (TOR), AMP kinase, sirtuins and the IGF-1 pathway (33).

One of the positive effects of DR, and which is probably related to the increased longevity, is an increased resistance to different stressors. This may be mediated by an overexpression of antioxidant response and cellular repair genes and DNA and by suppression of inflammatory pathways (34). In a clinical context, DR has been found to protect against acute stressors such as chemotherapy (35), acetaminophen poisoning (36) and oxidative stress induced by ischemia-reperfusion injury (IRI) (37).

Ischemia-reperfusion injury is caused by a temporary loss of blood flow with subsequent tissue perfusion. Multiple causes of tissue injury secondary to IR have been described, including the production of reactive oxygen species (ROS), inflammatory cell infiltration and impaired calcium homeostasis (38).

In the context of transplant surgery, IR is a significant cause of acute morbidity. In kidney transplants, blood flow is suspended after extracting the donor kidney; this is the ischemic phase which produces hypoxia, nutrient deprivation and the accumulation of metabolic products (39, 40). Once the kidney is implanted in the recipient, blood circulation is reestablished: the reperfusion phase. The arrival of oxygenated blood to a tissue subjected to ischemic stress increases the production of ROS, induces apoptosis and promotes the activation of the inflammatory response, producing increased tissue injury (41) with possible acute renal failure (PMID: 22045571), primary dysfunction (PMID: 12631369) and acute or chronic rejection (42). Preventing or reducing renal IR would improve the results of kidney and other transplants in general. Unfortunately, there is no effective intervention for this.

Due to the ever-increasing number of kidney transplant recipients and the low availability of kidney donors, increasingly older donors are being accepted in clinical practice, with a greater incidence of morbidities such as diabetes and obesity which make them more susceptible to IR . This leads to the need to develop interventions to improve the success rate of this type of transplants.

The Erasmus Medical Center experimental surgery group found that subjecting young 10-14 week old mice to a 30% CR protocol for two to four weeks was enough to improve survival and kidney function following IR. They also found that a three day fast induced the same level of

protection. In animals subjected to either of the two previously mentioned regimens, there was improved sensitivity to insulin, an increase in antioxidant defense markers and a decrease in inflammatory and IGF-1 signaling markers. The kidney transcriptome of these same mice showed enrichment in genes found in long-term CR, indicating that brief periods of CR or fasting are enough to activate the protective response (5). In order to determine the impact that this type of interventions could have on human health, the study must be extended to old and obese mice, which better represent the characteristics of the group of potential transplant donors and recipients. In the first part of this study, young and old mice were subjected to a three day fast. The level of protection of both groups was characterized, and the transcriptomic responses of both were determined.

In order for the protective phenotype against IR to be induced in humans, with the aim of improving organ transplantation results, alternative mechanisms to induce resistance to stress must be identified. A four-week CR protocol is difficult to adhere to, and fasting, even for short periods of time, may be counterproductive in post-transplant surgery recovery (37). In the second part of this research, the role of restriction of various macronutrients in the induction of protection against IR was studied. To do this, young mice were subjected to different diets restricting proteins, carbohydrates and fats. Once again, the level of protection of each of the experimental groups was characterized, and their transcriptomic responses were determined.

The aims of this research were the identification of transcriptomic response related to the protection against IRI in old mice and after different dietary modifications. To do that was necessary to establish the experimental models, to characterize the effect of the stress protection and generate the samples to quantify the global gene-level expression. A team of researchers of the Department of Surgery, Laboratory for Experimental Transplantation and Intestinal Surgery (LETIS), Erasmus University Medical Center, under the direction of Professor Ron de Bruin, developed all the processes oriented to answer the questions in this research. In order to increase the understanding of the transcriptomic analysis, and the implications of them, I provided in this report a short description of methods and results performed in parallel with the transcriptomic analysis. An integrate compendium of the methods and results described in this chapter are already published (43, 44).

This chapter is a result of the adaptation of two publications related to this thesis:
PMID: 24959849
PMID: 28102354

2.2 Methods

2.2.1. Mouse models

2.2.1.1. Aged mice: All aged mice were bred, raised and kept under identical standard laboratory conditions as described (PMID: 22953029). They were wild type FVB-C57BL/6J F1-hybrid mice, with an average age of 72 and 74 weeks and average weight of 47.3 grams, . Animals were allowed free access to water and food unless noted otherwise.

2.2.1.2. Young mice: C57BL/6 male mice, 10–12 weeks old (20–25 grams), were obtained from Harlan, the Netherlands. Animals were housed under standard conditions. All mice had ad libitum (AL) food and water except where specific dietary restriction protocols were applied.
All experiments were performed with the approval of the Animal Experiments Committee of the Erasmus University Medical Center, Rotterdam, the Netherlands under the Dutch National

Experiments on Animals Act and according to the ARRIVE Guidelines, Animal Research: Reporting of In Vivo Experiments (45).

2.2.2. Dietary interventions:

2.2.1. Control diet:

Three different control diet were used, they differed in the protein source. One diet consisted of crude protein and it was called “SDS”, other control diet consisted diet of lactic casein protein and it was called “Control” diet. Finally, a third control diet consisted of AIN93G synthetic pellets. The reason of the two first different control diets was the availability of the specific control diet in the moment that experiments were performed. Diet AIN93G was used in order to avoid the generation of bladder stones in Ercc1Δ/− mice . “SDS” diet was used in the evaluation of renal protection after 3 days of fasting in old mice. “Control” diet were used in the evaluation of the response of different type of dietary restrictions protocols.

2.2.2. Long-term dietary interventions:

At the start of the dietary intervention period, all mice were transferred to clean cages at 4:00 pm. Mice were randomly divided into a group with 30%DR (n = 5) or AL access to a carbohydrate-free (CHO-free) diet (n = 6) or a fat-free diet (n = 6) for 14 days, or a protein-free diet (n = 6) for 10 days. Mice in the control group for DR had AL access to the control SDS chow (n = 10), the control group for CHO-free and fat-free had AL access to the Control diet (n = 12). The effect of food intake was measured using pair-fed (PFed) control groups. Pair-feeding of each group was accomplished by giving the PFed groups the identical iso-caloric amount of the control diet as the mice on the experimental diet had consumed the day before. The CHO-free, fat-free and protein-free diets were PFed in this manner (n = 6/group). Mice with 30%DR were given 70% of the normal daily intake of mice on the control diet, which was administered once daily at 4:00 pm.

2.2.3. Short-term dietary intervention:

The same procedure was followed as for the long-term experiment. Mice were randomly divided into groups with AL access to control diet (n = 4), a protein-free diet (n = 6 per group) for three days or 30%DR for three days (n = 6), or into groups with AL access to SDS chow or fasting for three days (n = 5 per group).

2.2.3. Surgical procedure oriented to induce renal IRI:

Mice were anaesthetized by isoflurane inhalation. A midline abdominal incision was performed and the renal artery and vein of both kidneys were exposed. The pedicles of both kidneys were occluded for 37 minutes in males or 60 minutes in females, it was because female are more resistant to IRI. Purple discoloration of the kidneys confirmed ischemia macroscopically. After removal of the clamps, reperfusion was confirmed when the kidney color turned back to normal. The incision was closed in two layers. The mice used for microarray analysis did not undergo renal IRI, instead were sacrificed right after the dietary intervention.

2.2.4. Characterization of the renal phenotype after IRI:

The animals were followed up to 28 days postoperatively unless they died or were sacrificed as a result of morbidity (ruffled fur, decreased mobility, cold to the touch, excessive weight loss. During follow-up, they were inspected at least daily. At day 28, all remaining animals were

euthanized after which the abdominal cavity was opened for inspection of the kidneys. Serum urea and creatinine levels were measured using the QuantiChrom assay kits (DIUR-500 and DICt-500, Gentaur Europe, Brussels, Belgium). For assessment of the kidney function, the one-way ANOVA was used including the Bonferroni test for multiple comparisons. Means were compared using either the non-parametric Mann-Whitney U test or the independent t-test for parametric data. The survival curves were compared using the Log-rank (Mantel-Cox) test and visualized by the Kaplan-Meier curve.

Methods implemented by the author of this thesis

2.2.5. Transcriptomic analysis

It is a report of transcriptomic analysis of several experimental groups, with different interventions, ages, genotypes and organs. Table 1 summarize the samples used in this research to facilitate the tracking of the analysis.

A.

Dietary Intervention	Strain	Genotype	Age (weeks)	Number of arrays	Duration (days)	Organ measured
Control SDS AL	FVB-C57BL/6J	wt	72-74	5	3	Kidney
3-day fasting	FVB-C57BL/6J	wt	72-74	5	3	Kidney
Control SDS AL	FVB-C57BL/6J	wt	12-14	5	3	Kidney
3-day fasting	FVB-C57BL/6J	wt	12-14	5	3	Kidney

B.

Dietary Intervention	Strain	Genotype	Age (weeks)	Number of arrays	Duration (days)	Organ measured
Control SDS (control 2-week 30% DR)	C57BL/6	wt	10 -12	4	14	Kidney
2-week 30% DR	C57BL/6	wt	10 -12	5	14	Kidney
Control SDS (control 3-day fasting)	C57BL/6	wt	10 -12	5	3	Kidney
3-day fasting	C57BL/6	wt	10 -12	4	3	Kidney
Control	C57BL/6	wt	10 -12	5	3	Kidney
Protein-free	C57BL/6	wt	10 -12	5	3	Kidney
Fat-free	C57BL/6	wt	10 -12	4	3	Kidney
Carbohydrate-free	C57BL/6	wt	10 -12	5	3	Kidney

Table 1. Overview of gene transcription experiments. A. Samples used to identify the changes in the transcriptome of old mice after 3 days fasting. B. Experimental groups used to identify transcriptomic modifications associated to several dietary interventions. All the transcriptomic experiments were performed on male mice.

2.2.5.1. Total RNA extraction: Total RNA was extracted using QIAzol lysis Reagent and miRNAeasy Mini Kits (QIAGEN, Hilden, Germany), following Qiagen protocol. Addition of wash buffers RPE and RWT (QIAGEN) was done mechanically by using the QIAcube (QIAGEN, Hilden, Germany) via the miRNAeasy program. Isolated RNA was and stored at −80 °C. The concentration of RNA was measured by Nanodrop (Thermo Fisher Scientific™, Breda, the

Netherlands) and RNA quality was assessed using the 2100 Bio-Analyzer (Agilent Technologies, Amstelveen, the Netherlands) according to manufacturer's instructions. The RNA quality was expressed as the RNA integrity number (RIN, range 0–10). RIN values of included samples ranged between 6.6 and 8.5.

2.2.5.2. Microarray hybridization: Hybridization to Affymetrix HT MG-430 P.M Array Plates was performed at the Microarray Department of the University of Amsterdam according to Affymetrix protocols. Quality control was performed using the pipeline at the www.arrayanalysis.org website (Maastricht University)

2.2.5.3. Data pre-analysis: Raw data (CEL files) were normalized by robust multichip average (RMA) in the oligo BioConductor package, which summarizes perfect matches through median polish and collapses probes into core transcripts based on CDF annotation file provided by Affymetrix using the R open statistical package (http://www.r-project.org/). All data files have been submitted to the NCBI gene expression omnibus under accession number GSE65656, and GSE52982.

2.2.5.4. Principal component analysis: Principal component analysis (PCA) was performed using all the probe sets in the array. A graphical representation was generated to show the relationship among the different samples. PCA is a linear projection method that defines a new dimensional space to capture the maximum information present in the initial data set. It is an unsupervised exploratory technique used to remove noise, reduce dimensionality and identify common/dominant signals oriented to try to find biological meaning (46). The two principal components with the highest amount of variance were plotted. PCA was performed using the prcomp package and the plot was drawn with gplots, both from the Bioconductor project (https://www.bioconductor.org/).

2.2.5.5. Detection of differentially expressed genes (DEG): The linear model from Limma (47) implemented in R was used to identify the DEGs. Pairwise comparisons for each genotype between ad libitum and dietary restriction samples were applied to calculate the fold change (FC), P value and false discovery rate (FDR) for each probe in the microarray. Cut-off values for a DEG were put at FDR < 5% with FC ≥ |1.5| (absolute value). For all mouse analyses, differentially expressed probes were considered as DEGs.

2.2.5.6. Pathway analysis: Pathway enrichment analysis was conducted via overrepresentation analysis (ORA). ORA was performed in the Interactive pathway analysis (IPA) of complex genomics data software (Ingenuity Systems, Qiagen) or DAVID bioinformatics resources (https://david.ncifcrf.gov/) by employing a pre-filtered list of differentially expressed genes. Genes were selected as differentially expressed if they had a fold change≥ 1.5 and an FDR lower than 0.05. The over-represented canonical pathways were generated based on information in the Ingenuity Pathways Knowledge Base. A pathway was selected as deregulated when the P value in the Fisher test was lower than 0.01.

Additionally, IPA transcription factor (TF) analysis was performed to identify the cascade of upstream transcriptional regulators that can explain the observed gene expression changes in the different lists of DEGs. To do this, data stored in the Ingenuity Knowledge Base, with prior information on the expected effects between TF and their target genes, were used. The analysis examines how many known targets of each TF are present in the list of DEGs, and also compares their direction of change to what is expected from the literature, in order to predict likely relevant transcriptional regulators. If the observed direction of change is mostly consistent

with a particular activation state of the transcriptional regulator ('activated' or 'inhibited'), then a prediction is made about that activation state. For each TF two statistical measures are computed (overlap P value and activation z-score). The overlap P value labels upstream regulators based on significant overlap between data set genes and known targets regulated by a TF. The activation z-score is used to infer the likely activation states of upstream regulators based on comparison with a model that assigns random regulation directions. Overlap P value lower than 0.05 and z-score higher than |2| were selected as thresholds to identify a TF as relevant.

2.2.5.7. Determination of enrichment factor and P values of overlap: Overlap between lists of DEGs was identified looking by the intersection between pair of lists. To determine if the overlap was higher than expected by chance the hypergeometric distribution was used as is implemented in phyper function in R. Additionally the factor of enrichment was calculated with the formula: EF= nAB/((nA× nB)/nC). Where: nA = Number of DEG in experimental group A; nB = Number of DEG in experimental group B; nC= Number of total genes in the microarray; nAB= Number of common DEG between A and B.

2.2.5.8. Data integration by ranking meta-analysis: The methodology applied was combining rank orders. It is a non-parametric approach based on rank orders. The R package RankProd implemented in INMEX was used (48). In summary, for each dataset, the fold changes (FC) were calculated for all possible pairwise comparisons. The ranks of the fold changes within each comparison were used to calculate the rank product for each gene. To assess the null distribution of the rank product within each data set, a permutation test was performed. The process was repeated several times to compute the P-value and false discovery rate (FDR) associated with each gene.

2.3. Results and discussion

This section is divided into two sections. Each section describes the results and discussion of individuals sub-projects: 2.3.1 Transcriptomic analysis of kidney in aged mice after three days fasting, 2.3.2 Transcriptomic analysis of kidney in mice after several diets

2.3.1 Characterization of transcriptomic fasting response in old mice.

2.3.1.1. Preoperative fasting protects against renal ischemia-reperfusion injury in aged mice (43).

Preoperative fasting strongly increased the probability of survival after IRI. Mice under a normal diet had less than 10% of survival after 10 days of the damage. Indicating that IRI is a strong an almost lethal level of stress in normal conditions. Both male and female fasted mice had an important survival compared with AL fed mice (Figure 1).

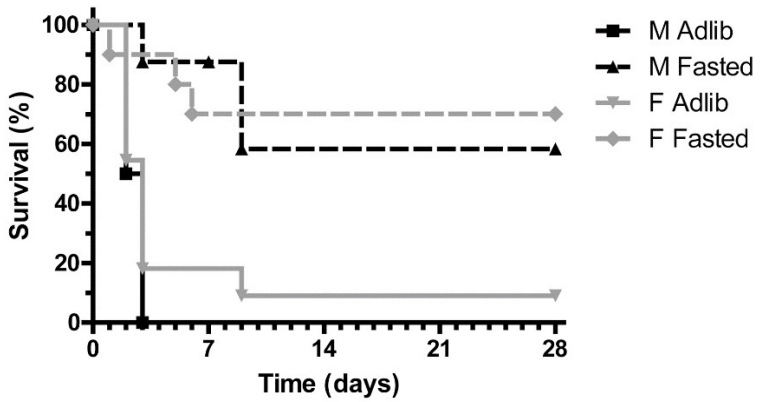

Figure 1. Survival curves of old mice after renal IRI with fasting or AL. Both fasted groups show a significantly improved survival: p=0.0171 for males, p=0.0040 for females. M=male, F=female, Adlib=ad libitum fed. (Modified from (43))

Fasting also protect the renal function after IRI, markers indicative of the renal function as serum urea and creatinine levels were lower compared with AL mice after IRI. Additionally there were detected an increase in the tubular epithelial regeneration, less necrosis and more regeneration in fasting mice that their counterparts with AL diet (43).

All results together indicated that fasting is able to activate the survival response that protect against renal IRI in old mice. Next, I explored the transcriptomic response and it was compared with the transcriptomic response of fasted young mice in order to detect how aging modified the response.

2.3.1.2. Kidneys of fasting old mice have an incomplete transcriptional response compared with the transcriptome of kidneys of fasting young mice

For this research were generated global transcriptome profiles from the kidneys of ten old male mice (72-74 weeks old) using Affymetrix microarrays. There was two experimental groups, five mice were under AL diet and the other five mice were under 3 days fasting. The quality of the microarrays were evaluated as is described in methods. All sample had high quality, then they were used in posterior analysis. Figure 2A shows the PCA plot of the samples. Samples in the same experimental group clustered together according the PC1. Two samples, one of each experimental group were located in the most negative part of PC2. Quality of those samples were re-checked, they had a similar quality compared with the other samples and the same date of hybridization, then there was no evidence that they have technical issues and it is probably related with biological variability of old mice.

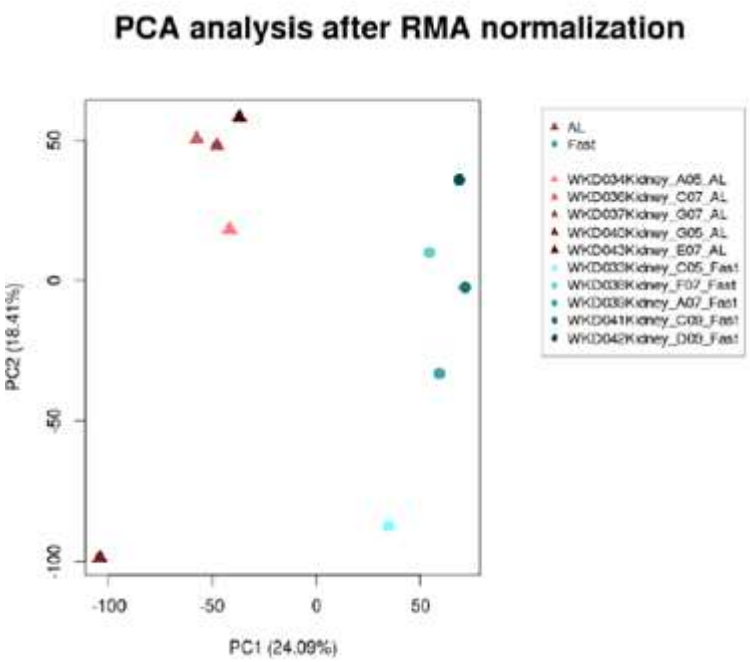

Figure 2. Principal component analysis (PCA) of microarrays from old mice. Unbiased representation of each microarray analyzed. Brown triangles represent AL samples; blue circles represent 3 days fasted samples. PC1 explain 24% of the total variability. Samples of each experimental group are located in different parts of PC1. Fasted samples are in positive part of PC while AL samples are in the negative region of PC1.

In a previous research was demonstrated that young mice fasting for three days have a complete protective response for renal IRI, the totality of mice survived (PMID: 19878145). Transcriptomic of four young mice after three days of fasting and four AL mice were studied in the same research. Those data were re-analyzed to compare the transcriptomic response after fasting in young mice with the response in old mice. Again, the raw files were evaluated by quality, all passed the control and they were used to posterior analysis. Figure 2B shows the PCA of those samples.

The ideal option to identify parallels and divergences among the response of old and young mice to fasting should be to analyze the samples simultaneously, but both datasets were hybridized in two different dates. Affymetrix is very sensitive to technical variations as the facility where they are processes, the person on charge or even the date of hybridization. Figure 2C shows the unbiased relation of the samples when both datasets were combined. The PC1 explaining the 50% of the variability is related with the day of hybridization and with the age of the mice but this to variables are connected. With this experimental setup is not possible to correct the batch effect then both datasets were processes independently.

Datasets were analyzed comparing fasting intervention with AL samples. Table 2 summarized the number of differentially expressed genes detected in both groups of age. There were three times more DEG in young mice compared with old mice. The proportion of down- and up-regulated genes were similar in both groups with a similar number of DEG in both directions.

Condition	DEG	Up	Down	EF
3dayFast-Old	854	454	400	13.1
3dayFast-Young	2408	1189	1219	

Table 2. Number of DEG in old and young fasting kidneys compared with AL kidneys.

Venn diagram (Fig. 3) shows that majority of probe sets (87%) found in aged mice overlap with the probe sets found in young mice. However, young mice have three-fold increase of significantly regulated genes indicative of a stronger, more extensive response to fasting in young compared to aged mice.

To know the extension of the similarity among both transcriptomic responses, the number of DEG in common were calculated (Fig 3). There were 296 up-regulated genes and 305 down-regulated genes in common. The 70% of total DEG after fasting in old mice were de-regulated with the same direction of the change in young mice. Enrichment factor (EF) also was calculated, this factor means how many times there are more genes in common than expected by chance. In the comparison of old and young response the EF was 13.1, with a p value lower than 1E-15.

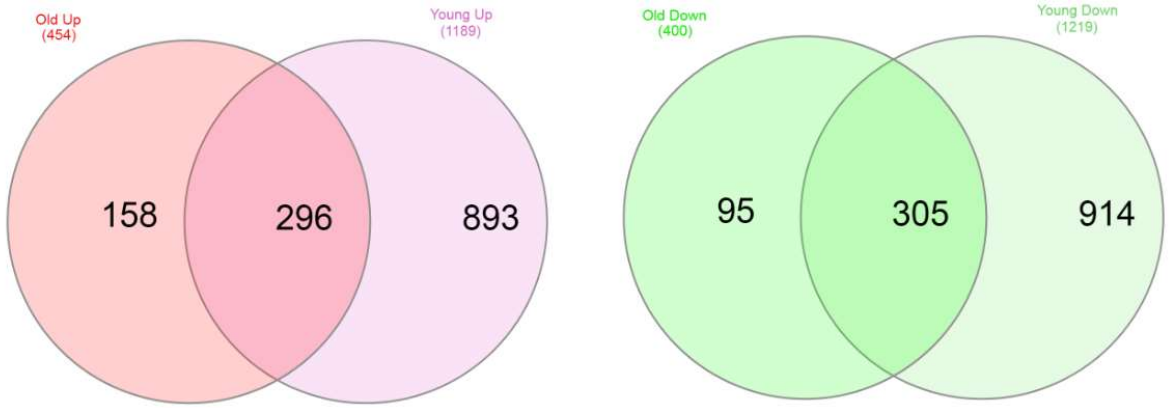

Figure 3. Venn diagram of the DEG, up- and down-regulated. Intersections shows the overlapping among old and young transcriptomic response.

To determine the effect on a biological level, pathway overrepresentation analyses of DEG were performed with the clustering algorithm implemented in DAVID. This approximation identified de-regulated pathways and they are clustered together if they have overlapping genes, then the interpretability of the result is more direct. The database pathways used in this analysis were KEGG and the Gen-Ontology biological process. The DEG were divided in up-regulated genes and down-regulated genes. Independent pathway analysis was performed with the set of list generated. The advantage of this approximation is that it incorporates the direction of the de-regulation of the pathway. Table 3 and table 4 show the statistically significant de-regulated pathways.

Pathway analysis on up-regulated genes in aged and young mice resulted in several clusters of de-regulated pathways in common (Table 3). There are up-regulation of pathways related with metabolism of fatty acid compose (cluster 1 in both lists), metabolism of xenobiotics and glutathione metabolism (cluster 3 in both lists) and lipid storage (cluster 3 in both lists). Others pathways were de-regulated only in old or young mice. The specific pathways de-regulated in

young mice were cholesterol metabolic process (cluster 2) and TGF-beta signaling pathway (cluster 5). The pathways up-regulated only in young mice are pathways related with stress response as cellular response to DNA damage stimulus and negative regulation of apoptosis.

A.

Up Old

Cluster 1

Category	Term	Count	FE	PValue
KEGG	PPAR signaling pathway	14	9.2	2.57E-09
KEGG	**Fatty acid degradation**	**11**	**11.7**	**1.95E-08**
KEGG	Peroxisome	12	7.6	3.96E-07
GO_BP	**fatty acid beta-oxidation**	**8**	**11.7**	**4.54E-06**
KEGG	**Fatty acid metabolism**	**7**	**7.2**	**3.76E-04**

Cluster 2

Category	Term	Count	FE	PValue
GO_BP	cholesterol metabolic process	8	5.8	4.53E-04
GO_BP	cholesterol homeostasis	6	6.2	0.0029

Cluster 3

Category	Term	Count	FE	PValue
KEGG	**Metabolism of xenobiotics by cytochrome P450**	**7**	**5.7**	**0.0013**
KEGG	**Drug metabolism - cytochrome P450**	**7**	**5.5**	**0.0015**
KEGG	**Glutathione metabolism**	**5**	**4.8**	**0.0201**

Cluster 4

Category	Term	Count	FE	PValue
GO_BP	**lipid storage**	**5**	**12.0**	**7.36E-04**
GO_BP	**positive regulation of sequestering of triglyceride**	**3**	**27.7**	**0.0047**
GO_BP	**lipid particle organization**	**3**	**12.9**	**0.0218**

Cluster 5

Category	Term	Count	FE	PValue
KEGG	TGF-beta signaling pathway	8	4.9	0.0011
KEGG	Signaling pathways regulating pluripotency of stem cells	9	3.4	0.0046

B.

Up
Young

Cluster 1

Category	Term	Count	FE	PValue
KEGG	**Fatty acid degradation**	**14**	**6.0**	**2.60E-07**
GO_BP	**fatty acid beta-oxidation**	**11**	**6.4**	**5.75E-06**
KEGG	Biosynthesis of unsaturated fatty acids	8	6.3	1.92E-04
KEGG	**Fatty acid metabolism**	**8**	**3.3**	**0.0095**
KEGG	alpha-Linolenic acid metabolism	5	4.2	0.0281

Cluster 2

Category	Term	Count	FE	PValue
GO_BP	**circadian rhythm**	20	4.7	3.45E-08
GO_BP	circadian regulation of gene expression	10	4.2	5.64E-04

Cluster 3

Category	Term	Count	FE	PValue
KEGG	**Drug metabolism - cytochrome P450**	**13**	**4.2**	**4.98E-05**
KEGG	**Metabolism of xenobiotics by cytochrome P450**	**12**	**4.0**	**1.73E-04**
KEGG	**Glutathione metabolism**	**10**	**3.8**	**9.73E-04**

Cluster 4

Category	Term	Count	FE	PValue
GO_BP	**lipid particle organization**	**6**	**10.2**	**1.94E-04**
GO_BP	**positive regulation of sequestering of triglyceride**	**4**	**14.6**	**0.0018**
GO_BP	**lipid storage**	**6**	**5.7**	**0.0035**

Cluster 5

Category	Term	Count	FE	PValue
GO_BP	response to UV	10	5.4	7.21E-05
GO_BP	cellular response to DNA damage stimulus	25	1.5	0.0406

Cluster 6

Category	Term	Count	FE	PValue
GO_BP	negative regulation of apoptotic signaling pathway	6	6.1	0.0025
GO_BP	negative regulation of endothelial cell apoptotic process	5	4.6	0.0224

Table 3. Pathways over-represented in the list of up-regulated genes. The analysis was performed with Gen-Ontology biological process and KEGG databases. Count means the number of DEG in the pathway, FE the number of times that there are more genes than

expected by chance. Pathways in bold are the common pathways de-regulated in old and young groups.

Amongst the de-regulated pathways in the list of down-regulated genes, the most altered pathways in old and young mice were steroid and cholesterol biosynthetic process (cluster 1 and 2 in table 4A and 4B) , steroid biosynthetic process and lipid metabolic process (Table 4). Additionally, the down-regulated genes in old mice had a wider pathways de-regulation compared with young mice. The specific pathways de-regulated in old mice were Cellular communication (Table 4B cluster 3), immune related pathways (Table 4B cluster 5 and 8) and RNA splicing (Table 4B cluster 7) among others.

A.

Down Old

Cluster 1

Category	Term	Count	FE	PValue
GO_BP	lipid metabolic process	21	3.1	1.45E-05
GO_BP	**steroid biosynthetic process**	**6**	**15.2**	**3.96E-05**
GO_BP	**cholesterol biosynthetic process**	**6**	**12.8**	**9.32E-05**
KEGG	**Steroid biosynthesis**	**4**	**12.4**	**0.0038**

Cluster 2

Category	Term	Count	FE	PValue
GO_BP	**cholesterol biosynthetic process**	**6**	**12.8**	**9.32E-05**
GO_BP	**isoprenoid biosynthetic process**	**4**	**16.1**	**0.0018**
KEGG	**Terpenoid backbone biosynthesis**	**4**	**10.2**	**0.0065**

B.

Down Young

Cluster 1

Category	Term	Count	FE	PValue
GO_BP	**steroid biosynthetic process**	**14**	**5.0**	**3.25E-06**
KEGG	**Steroid biosynthesis**	**8**	**8.6**	**1.88E-05**
GO_BP	**cholesterol biosynthetic process**	**9**	**6.2**	**6.83E-05**
GO_BP	**cholesterol biosynthetic process**	**14**	**3.7**	**9.78E-05**

Cluster 2 Enrichment Score: 3.496538729728804

Category	Term	Count	FE	PValue
GO_BP	**GO:0006695~cholesterol biosynthetic process**	**9**	**6.2**	**6.83E-05**
KEGG	**mmu00900:Terpenoid backbone biosynthesis**	**7**	**6.2**	**6.42E-04**
GO_BP	**GO:0008299~isoprenoid biosynthetic process**	**6**	**7.8**	**7.39E-04**

Cluster 3 Enrichment Score: 2.047875076022803

Category	Term	Count	FE	PValue
KEGG	mmu04512:ECM-receptor interaction	12	2.8	0.0035
KEGG	mmu04510:Focal adhesion	20	2.0	0.0058
KEGG	mmu04151:PI3K-Akt signaling pathway	26	1.5	0.0357

Cluster 4	Enrichment Score: 1.6786400505292474			
Category	Term	Count	FE	PValue
KEGG	mmu00860:Porphyrin and chlorophyll metabolism	8	4.0	0.0033
GO_BP	GO:0033014~tetrapyrrole biosynthetic process	3	13.2	0.0187

Cluster 5	Enrichment Score: 1.6275706754998545			
Category	Term	Count	FE	PValue
KEGG	mmu04610:Complement and coagulation cascades	11	3.0	0.0036
KEGG	mmu05020:Prion diseases	7	4.3	0.0047
GO_BP	GO:0006958~complement activation, classical pathway	7	2.8	0.0374

Cluster 6	Enrichment Score: 1.6016409696833063			
Category	Term	Count	FE	PValue
GO_BP	GO:0042759~long-chain fatty acid biosynthetic process	4	9.8	0.0063
KEGG	mmu01040:Biosynthesis of unsaturated fatty acids	6	4.5	0.0089
KEGG	mmu01212:Fatty acid metabolism	8	3.2	0.0112
GO_BP	GO:0006636~unsaturated fatty acid biosynthetic process	4	5.9	0.0280

Cluster 7	Enrichment Score: 1.3488440421168715			
Category	Term	Count	FE	PValue
GO_BP	GO:0051028~mRNA transport	12	3.0	0.0020
GO_BP	GO:0008380~RNA splicing	17	1.6	0.0819

Cluster 8	Enrichment Score: 1.242051379097638			
Category	Term	Count	FE	PValue
GO_BP	GO:0019882~antigen processing and presentation	8	3.3	0.0106
GO_BP	GO:0051085~chaperone mediated protein folding	4	6.8	0.0188
KEGG	mmu05310:Asthma	5	4.3	0.0273

Cluster 9	Enrichment Score: 0.8639624899801572			
Category	Term	Count	FE	PValue
GO_BP	GO:0007029~endoplasmic reticulum organization	5	4.1	0.0320

Table 4. Pathways over-represented in the list of down-regulated genes. The analysis was performed with Gen-Ontology biological process and KEGG database. Count means the number of DEG in the pathway, FE the number of times that there are more genes than expected by chance. Pathways in bold are the common pathways de-regulated in old and young groups.

2.3.1.3 Discussion

Dietary interventions as DR and fasting induces an increased resistance to several types of acute stress (49, 50). Several mechanism have been linked to this protective phenotype as attenuation of oxidative stress, up-regulation of stress proteins, reduce inflammation and reduce IGF-1 signaling (5). In a clinical context, a cause of acute stress is IRI, it is a relevant cause of morbidity and mortality related to vaso-occlusive disease and organ transplantation. The damage caused by renal IRI in animal models is severe and lethal in the majority of the cases. Short time DR or three days fasting increases dramatically the protection of young mice against renal IRI, with a 100% of survival (5). It is important to know if fasting is able to induce the protective response in aged organisms because most of the people expose to IRI are old. We found that 3 days fasting induces the protective response in old mice, but compared to young mice the survival after renal IRI was 60% instead a 100% of survival described in young mice (5, 43).

We performed a transcriptomic analysis of kidneys of old and young mice after three days of fasting to identify how the protective response is modified by the age. Old and young datasets were analyzed independently because they were hybridized in different dates. First, a multidimensional reduction technique –PCA- was used to visualize the relation among the samples in each dataset. The PCA plot with the two more relevant PCs, showed that samples from older mice has a higher intra-group variability compared with samples from young mice. Transcriptional noise had been described in analysis of individual aged cells. Cells from older individuals had increased expression heterogeneity and variability (51), a plausible explanation, is that older individuals had been a longer time accumulating mutations in a stochastic way then it is expected the presence of more transcriptional noisy in tissues from old animals compared with young animals (52).

Identification of DEG showed that the coordinate transcriptomic response in older mice is smaller in the number of genes compared with young mice. There were three times more DEG induced by fasting in young mice than the induced in old mice. However, the overlapping among the responses where high, with 13 times more DEG in common than expected by chance and 70% of DEG in old mice also DEG in young. When independent Affymetrix studies are compared, even they analyzed the same phenotype, the overlap is typically lower than 10% of the DEG (53). This result indicate the good quality of the data and that a proportion of the transcriptomic response is conserved with aging.

To have a better understanding of the biological processes modulated by fasting an over-representation pathways analysis was performed. Up-regulated and down-regulated genes were studied in an independent analysis to improve the statistical power and to increase the number of detected pathways (54). In the list of up-regulated genes in old mice (Table 3A), five clusters of pathways were identified. Cluster 1, 2 and 4 contains pathways related with fatty acid degradation, beta-oxidation, cholesterol homeostasis and lipid storage. Those de-regulated pathways are related with the re-design of metabolic processes oriented to reduced fat synthesis and storage and increased oxidation in order to burn fat for the production of energy (55). The same clusters with the same pathways were detected in the up-regulated genes in young mice (Table 3B). The overlapping in these clusters indicated that the change in the metabolism is similar with the age and both group of age had a similar level of deprivation of nutrients. Other common up-regulated group of pathways was located in the cluster 3 (Table3A and 3B) and includes metabolism of xenobiotics by cytochrome P450 and glutathione metabolism. This cluster is compose by pathways related with increased resistance to stress reducing the levels of oxidative stress (56, 57). It is probably the central pathway related with

the increases of the resistance to renal IRI in old mice but not the only in young mice. Cluster five, composed by TGF-beta signaling pathway was uniquely de-regulated in old mice (Table 3A). Activation of this pathway had been linked with the regulation of NOX2/NOX4 expression and increased cerebral IRI (58), the up-regulation also is related with renal fibrosis (58). It is possible the activation of TGF-β could be related with the non-complete protection of fasting in old mice but this hypothesis need more validation.

The analysis of down-regulated genes was also informative about the parallels and divergences among the transcriptional response in old and young mice. All the pathways down-regulated in old mice were also down-regulated in young mice. Those pathways were located in cluster 1 and 2 (Table 4A and 4B) and they were related with the synthesis of steroids and cholesterol; those pathways are connected with the re-design of the metabolic network in absence of food. Young mice had a more extensive pathways down-regulated grouped in clusters 3 to 9 (Table 4B). The pathways represented in those clusters were indicative of a down-regulation of the immune response, protein folding and endoplasmic reticulum organization, all of them previously linked to protective response for previous studies (5, 59, 60).

In summary, this research shown that fasting induces non-global protection against renal IRI in aged mice. In concordance with that, the transcriptomic response is smaller in old mice compared with young mice. The majority of the pathways de-regulated in old mice are also de-regulated in young mice. However, the transcriptomic of young mice revealed the de-regulation of additional pathways related with increase of stress protection. Possible explanations of those differences only could be speculative with the actual evidence. Several hypothesis can propose: Aged organs are not able to activate a vigorous response because their functional reserve are diminished, the chronic low stress of aging itself could induces the partial activation of the response, aged organs need more time to activated the complete response.

Several experimental approximations could help to answered some of the raising questions, time series to evaluated the progression of the fasting response day by day in young and old mice and identification which of the old mice have the protective response (survival after renal IRI) and which one does not have protective response previous to the transcriptomic analysis.

2.3.2 A signature of renal stress resistance induced by short-term dietary restriction, fasting, and protein restriction (44)

2.3.2.1 Short time restriction of dietary protein induces protection against renal IRI

To determine the effect of short-term macronutrient deficiency on renal IRI, male mice were fed by three days with regimens of protein-free, carbohydrate (CHO)-free and fat-free diets before inducing renal IRI.
Only the protein-free diet improved survival (Fig. 4) and kidney function following renal IRI (44). Previously was showed that 30% DR for two weeks or 3 days fasting induce complete protection against renal IRI (5). Additionally, 30% DR for three days did not differ from mice fed ad libitum (37).

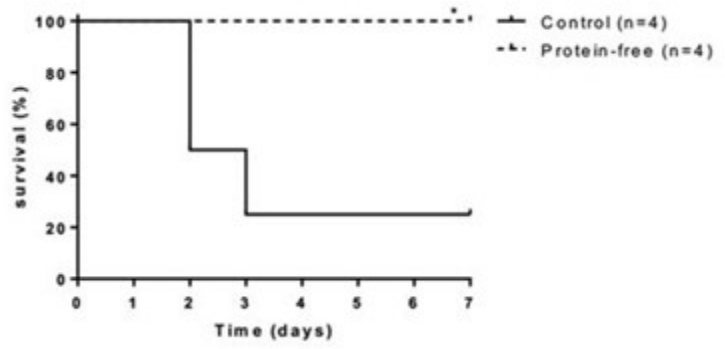

Figure 4. Survival curves of mice fed with protein free diet or AL. Three days of protein-free diet improved survival compared with AL fed controls. Adapted from (44).

Then, there are dietary interventions able to induce the protective response: 30% DR for two weeks, three days fasting or protein restriction diet. In addition, there are dietary interventions that do not induce a protective response: three days of 30% DR, CHO restriction or fat restriction.

The analysis in combination of all those dietary interventions will be informative to detect what are the genes in the core of the protective response. Transcriptomic data were obtained for all those experimental groups, as is summarized in table 1B.

2.3.2.2. Combined transcriptomic analysis of macronutrient-free diets, fasting and DR

The transcriptomic response of the kidney after protective diets: 3-days of fasting, two weeks of 30%DR, three days of protein restriction, and non-protective diets: three days of 30%DR, fat restriction or CHO restriction diet were analyzed by an Affymetrix microarray with 45,141 probes (HT MG-430 P.M). Each experimental group was compared to its corresponding AL fed control group (Table 1B). All microarrays were evaluated by quality, all of them passed it and then they were used for posterior analysis.

The complexity of the experimental setup made necessary to explore different strategies to do the analysis, first, the unbiased correlation of the samples was determinate by PCA (Fig. 5). The first obstacle to perform an integrate analysis of the data was the different day of hybridization of the samples. Affymetrix chips are sensible to hybridization conditions; different dates even in the same laboratory facility produce important technical variability. In the particular case of the data in this study the three day fast samples (control and experimental) were located in the positive part of the PC1 and precisely those samples were hybridized in a different date (Fig. 5). I performed several batch correction strategies (results not shown) but it was not possible to correct it, then this dataset was analyzed in an independent way. In the same PCA, control samples (white triangles and squares) and fat free diet samples are located close an indicator of fat free diet does not induced an important transcriptional response. The other samples are nor clearly separated, CHO free diet samples are located in similar positions of DR diets samples (3 days or 2 weeks).

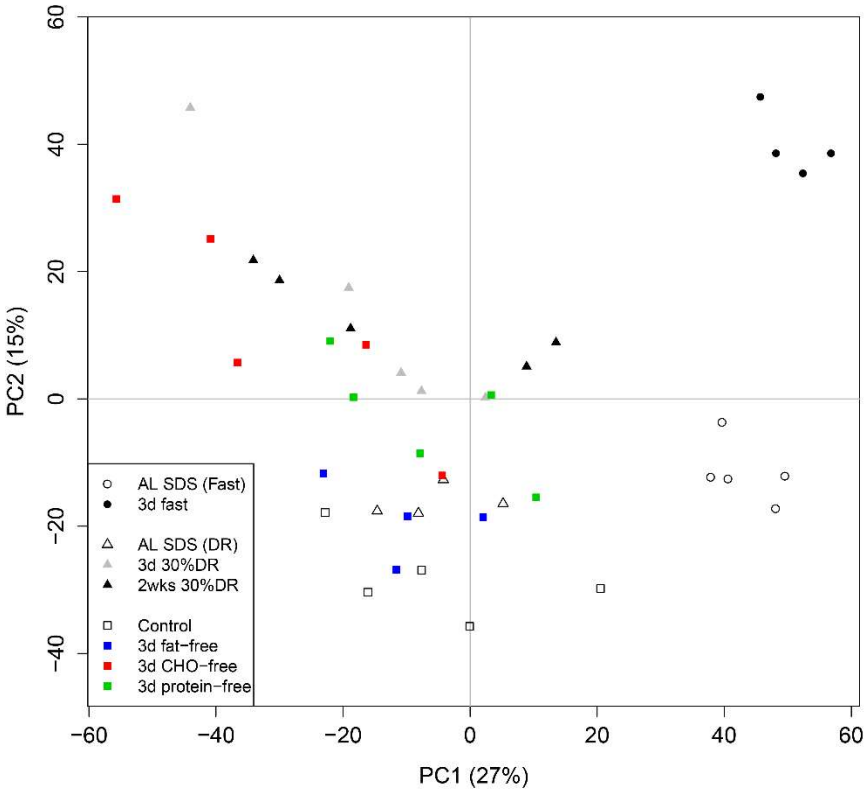

Figure 5. Unbiased graphical representation of PCA of all samples in the study. The largest source of variability in the study is represented by the PC1 (27%). The 3-day fasting group and their corresponding control group were hybridized on a different date than the other groups. This result made the joint analysis of all datasets impracticable. PC2 explains 15% of the variability, and it is related to the dietary interventions compared to the control samples. Adapted from (44).

Next, the DEG were determined, Table 5 summarize the number and direction of the change of the DEG for each dietary intervention. The highest number of DEG was found after three days of fasting. Two weeks of 30% CR induced five times lower number: 492 DEG. Three days of protein-free diet induced 391 DEG. Of the non-protective diets, the 3-day fat-free diet did not induce any DEPS when compared to control diet fed mice, while, according with the PCA analysis, three days of a CHO-free diet induced 1,717 DEPS. Three days of 30% CR resulted in 454 DEPS.

Dietary Intervention	DEG	Up	Down
3-day fasting	**2604**	**1268**	**1336**
2-week 30% DR	**492**	**265**	**227**
3d 30% DR	454	284	170
Protein-free	**391**	**230**	**161**
Carbohydrate-free	1717	613	1104
Fat-free	0	0	0

Table 5. Number of DEG induced after dietary interventions. All comparison were performed with samples obtained from mice fed with control diet. Protective diets are in bold.

Because the PCA (Fig. 5) suggested there are shared transcriptomic modifications in common among different dietary interventions, an overlapping analysis of DEG was performed. The number of DEG in common was calculated for each possible combination of interventions,. This analysis had in account the direction of the change, and then the overlapping genes indicate the same transcriptional response.

Comparison	Overlapping DEG	EF	P-value
2wks 30%DR vs. 3d 30%DR	195	39.4	3.44E-270
Protein-free vs. 3d 30%DR	116	29.5	2.22E-138
Protein-free vs. 2wks 30%DR	95	22.3	1.15E-99
Protein-free vs. Fasting	222	9.8	5.27E-169
2wks 30%DR vs. Fasting	247	8.7	8.88E-171
3d 30%DR vs. Fasting	208	8.7	3.12E-156
2wks 30%DR vs. CHO-free	122	8.2	5.71E-76
Protein-free vs. CHO-free	113	6	5.84E-55
Fasting vs. CHO-free	584	5.9	3.73E-300
3d 30%DR vs. CHO-free	107	5.8	8.66E-48

Table 6: Comparison of the overlapping DEPS between the five dietary interventions and their corresponding P-value and enrichment factor. The enrichment factor indicates the number of times the overlapping DEG is higher than expected by chance. All diets showed a significantly overlapping number of DEG, as shown by the corresponding p-values in the last column. Adapted from (44)

The highest percentages of EF were found between two weeks of 30%DR, three days of 30%DR and protein-free diet. Because the number of DEG in fasting is high, the EF are smaller but even there are similarities among fasting and protein free, and DR interventions. Interestingly, the non-protective CHO free diet has EF from 5.8 to 6.0 with the other protective diets. This result revealed several characteristics of the transcriptomic response to dietary interventions: first, there is a common transcriptional response in general (protective and non-protective diets). Second, two weeks of 30%DR and 3 days 30%DR induces a similar response. It is probably that the transcriptional response that 3 days 30%DR induces is incomplete and there are some additional genes induces by two weeks of 30%DR needed to confer the protection. Third, protein-free diet and two weeks of 30%DR had the higher level of EF (39.4) indicating that protein restriction induces a similar protection response than DR but quicker.

In order to improve the description of the relation among the transcriptomic response of the dietary interventions an additional analysis were performed. Since the 3-day fasting dataset was hybridized on a different date and it caused a stronger effect than the biological signal (Fig. 5). It was therefore not possible to integrate all complete datasets in one analysis. As a solution, we assumed 3-days of fasting to represent the widest transcriptomic protective response. It is supported with the overlapping analysis where fasting had the higher number of DEG in

common with the other diets. Then, all data sets were limited to its highest number of 2,604 DEG. This list of DEG was used for a principal component analysis (PCA) among the macronutrient free diets, two weeks-, and three days 30%DR and their control diets (Fig. 6).

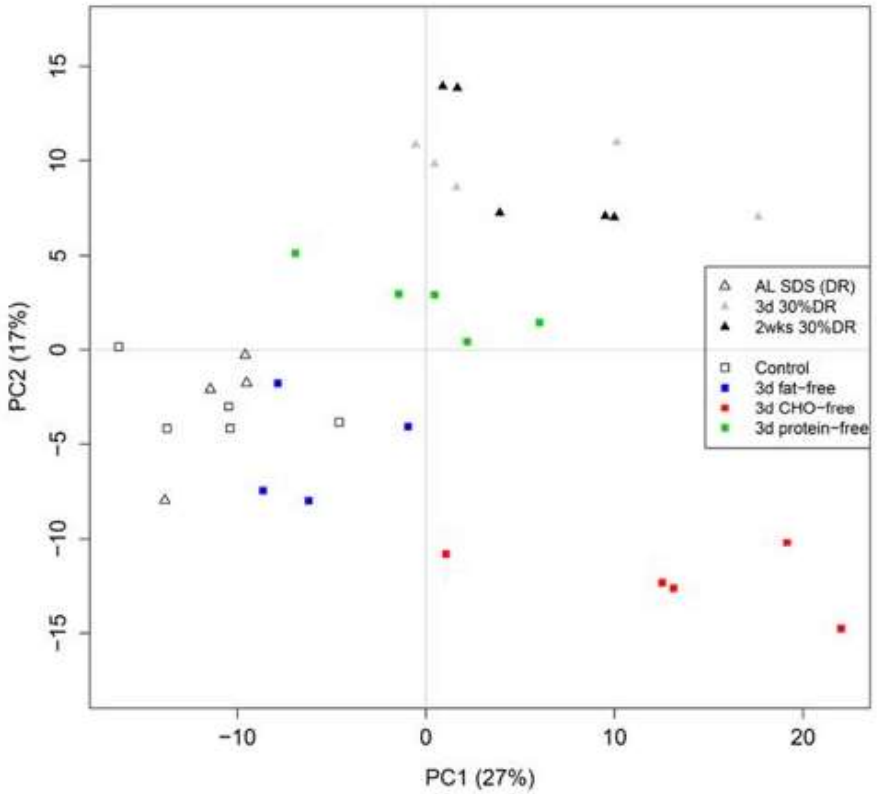

Figure 6. Principal component analysis (PCA) plot, based on the 2604 significantly DEG after three days fasting. The two control diets samples clustered together in the negative part of PC1 and neutral region of PC2. Fat free diet samples are located in the same region according with the evidence that this diet did not induce a transcriptional response. Both two weeks 30%DR and three days of 30%DR diet clustered close to each other. The protein-free diet had its own cluster, between control and DR samples. Three days of CHO-free diet samples were positioned far of the other samples. Adapted from (44).

When the PCA is limited to DEG after 3 days fasting the distribution of the samples are more informative respect the phenotype induced by them. The protective interventions were clustered close and the non-protective CHO-free diet samples were located far of the other interventions. Again, DR interventions does not matter the time of exposition had a similar transcriptomic response.

To compare the transcriptomic responses of protective interventions, all DEG were visualized in a Venn diagram (Fig. 7). This revealed 70 overlapping DEG in the three protective diets. Numbers of overlapping genes appeared too small to perform pathway analysis with the aim to find a common denominator of protection against renal IRI, and therefore an alternative approximation for analysis should be used.

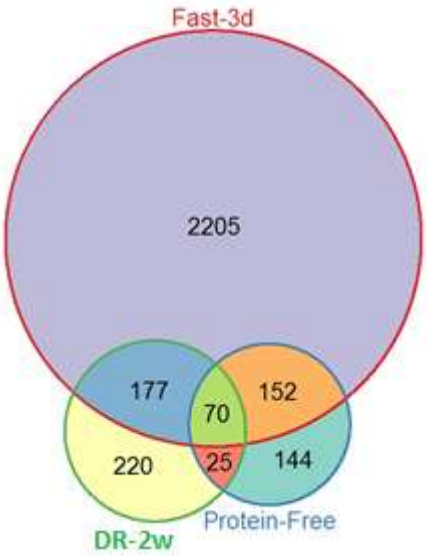

Figure 7. Venn diagram with the DEG of protective diets. The complete list of DEG for each protective diet were used in this analysis. Intersection of sets represent only DEG with the same direction of change.

Until now, taking together all the results: The data has difficulties to be analyzed because the batch effects and the complexity of the phenotype. The transcriptomic response to protective and non-protective diet is similar, but the PCA analysis was able to show that there are also differences. Fasting induces the more important transcriptional regulation and most of the genes de-regulated by this intervention are also de-regulated by the others interventions.

2.3.3.2 Pathway analyses of individual dietary interventions

To explore the biological value of these transcriptomic responses, we used an individual approximation to identify significantly enriched pathways as were determinate by Ingenuity analysis. The highest enriched pathways after the different dietary interventions were ranked by their –log p-value and summarized in Table 7. No clear pattern in overlapping pathways between all diets, or between the protective diets and the non-protective CHO-free diet, was observed. One pathway that emerged was the NRF2-mediated oxidative stress response pathway, since this pathway was activated by four out of five dietary interventions (Table 7) except by protein-free diet.

3-day FASTING

Canonical Pathway	**P-value**	**Genes Ratio**
Superpathway Cholesterol Biosynthesis	3.41E-08	14/87 (16.1%)
Cholesterol Biosynthesis I / II / III	2.18E-06	8/40 (20.0%)
LXR / RXR Activation	2.20E-06	27/139 (19.4%)
NRF2-mediated Oxidative Stress Response	6.27E-06	34/195 (17.4%)
LPS/IL-1 Mediated Inhibition of RXR Function	7.46E-06	39/245 (15.9%)
Acute Phase Response Signaling	7.24E-05	30/181 (16.6%)

GADD45 Signaling	1.25E-04	8/24 (33.3%)
AMPK Signaling	1.25E-04	25/180 (13.9%)
VDR/RXR Activation	2.18E-04	17/88 (19.3%)
Xenobiotic Metabolism Signaling	3.00E-04	42/304 (13.8%)

2-week 30% DR

Canonical Pathway	**P-value**	**Genes Ratio**
Circadian Rhythm Signaling	1.41E-05	6/38 (15.8%)
Aldosterone Signaling Epithelial Cells	3.20E-05	11/168 (6.5%)
Guanosine Nucleotides Degradation II	7.85E-04	3/22 (13.6%)
Urate Biosynthesis	1.01E-03	3/22 (13.6%)
Phenylalanine Degradation IV	1.27E-03	3/39 (7.7%)
2-ketoglutarate Dehydrogenase Complex	1.48E-03	2/9 (22.2%)
Adenosine Nucleotides Degradation II	1.57E-03	3/26 (11.5%)
NRF2-mediated Oxidative Stress Response	2.39E-03	9/195 (4.6%)
Protein Ubiquitination Pathway	2.63E-03	11/270 (4.1%)
Purine Nucleotides Degradation II	2.71E-03	3/35 (8.6%)

3-day PROTEIN-FREE

Canonical Pathway	**P-value**	**Genes Ratio**
Intrinsic Prothrombin Activation Pathway	5.18E-04	4/37 (10.8%)
Superpathway Cholesterol Biosynthesis	6.79E-04	4/87 (4.6%)
LPS/IL-1 Mediated Inhibition of RXR Function	8.81E-04	10/245 (4.1%)
Mevalonate Pathway I	9.87E-04	3/29 (10.3%)
Creatine-phosphate Biosynthesis	1.77E-03	2/9 (22.2%)
Superpathway of Geranylgeranyl	2.02E-03	3/37 (8.1%)
PXR/RXR Activation	2.12E-03	5/92 (5.4%)
GADD45 Signaling	2.35E-03	3/24 (12.5%)
Tryptophan Degradation	4.84E-03	2/18 (11.1%)
Nicotine Degradation II	9.33E-03	4/85 (4.7%)

3-day CARBOHYDRATE-FREE

Canonical Pathway	**P-value**	**Genes Ratio**
Histamine Degradation	9.52E-05	6/29 (20.7%)

Pyrimidine Deoxygenase De Novo Biosynthesis I	1.57E-04	6/34 (17.6%)
Superpathway of Serine and Glycine Biosynthesis I	2.57E-04	4/18 (22.2%)
Glycolysis I	6.98E-04	7/41 (17.1%)
NRF2-mediated Oxidative Stress Response	8.17E-04	24/195 (12.3%)
Cholesterol Biosynthesis I / II / III	1.04E-03	5/40 (12.5%)
Colanic Acid Building Blocks Biosynthesis	1.52E-03	5/36 (13.9%)
Fatty Acid β-oxidation	1.52E-03	5/21 (23.8%)
Protein Ubiquitination Pathway	1.58E-03	30/270 (11.1%)
Folate Transformations I	1.84E-03	4/32 (12.5%)

3-day 30% DR

Canonical Pathway	**P-value**	**Genes Ratio**
Dopamine Degradation	1.08E-04	5/35 (14.3%)
Aryl Hydrocarbon Receptor Signaling	1.37E-04	9/140 (6.4%)
LPS/IL-1 Mediated Inhibition of RXR Function	2.48E-04	11/221 (5.0%)
PXR/RXR Activation	2.63E-04	6/65 (9.2%)
Circadian Rhythm Signaling	1.03E-03	4/33 (12.1%)
NRF2-mediated Oxidative Stress Response	1.42E-03	9/193 (4.7%)
Tyrosine Degradation I	1.82E-03	2/5 (40.0%)
Histamine Degradation	2.09E-03	3/19 (15.8%)
Noradrenaline and Adrenaline Degradation	2.14E-03	4/40 (10.0%)
Adipogenesis Pathway	2.52E-03	7/134 (5.2%)

Table 7. Top 10 over-represented canonical pathways after fasting, dietary restriction and macronutrient free diets individually ranked by their –log P-value. Analysis revealed no pathways regulated in common between the three protective diets. Genes ratio is the number and percentage of genes differentially expressed in ratio to the total number of genes involved in the pathway. Adapted from (44).

Independent analysis identified pathways related to increased stress resistance as NRF2-mediated Oxidative Stress Response, LXR / RXR Activation and GADD45 signaling. Again, the individual analysis of de-regulated pathways was not informative about specific pathways de-regulated specifically and in common with protective diets. An explanation of that could be that each protective intervention induces a different protective response but EF analysis and PCA in figure 5 suggested a common transcriptional response.

2.3.3.3 Meta-analysis of protective transcriptomic responses

To further identify a common protective response and dissect it from the response of the non-protective CHO-free diet, a more comprehensive approximation was used. Meta-analysis of

combining rank orders methodology was implemented to prevent bias of the results based on different dates of hybridization as well as the stronger transcriptomic response after three days of fasting (48). The meta-analytic combination of the transcriptome of protective diets yielded 640 DEG. The DEG in common showed a similar fold change and directionality among the three protective dietary interventions.

Pathway	P-value	Z-score
LXR/RXR Activation	7.24E-09	0.302
FXR/RXR Activation	3.63E-06	1.045
LPS/IL-1 Mediated Inhibition of RXR Function	2.24E-05	−2.646
Superpathway of Cholesterol Biosynthesis	2.40E-05	N/A
NRF2-mediated Oxidative Stress Response	3.72E-05	2.24
Aryl Hydrocarbon Receptor Signaling	5.13E-05	1.633
PXR/RXR Activation	9.12E-05	1.594
Noradrenaline and Adrenaline Degradation	5.25E-04	N/A
Superpathway of Cholesterol Biosynthesis	2.23E-03	N/A
Glutathione-mediated Detoxification	2.47E-03	1.506
Intrinsic Prothrombin Activation Pathway	3.47E-03	N/A
Circadian Rhythm Signaling	3.59E-03	N/A
Retinoate Biosynthesis I	3.91E-03	N/A
Superpathway of Geranylgeranyldiphosphate Biosynthesis I	3.98E-03	N/A

Table 8. The top 10 overrepresented pathways derived from the 640 DEG in common between 3-days of fasting, 2 weeks 30%DR and 3 days of a protein-free. These pathways are mostly involved in regulation of nuclear receptor signalling (5 out of 10), biosynthesis signalling (2 out of 10) and cellular stress and injury (2 out of 10). Adapted from (44).

A pathway analysis of these DEG (Table 8) identified de-regulation de pathways related con inhibition of cellular stress and injury and biosynthesis pathways. Adding the 3-day 30%DR diet in the meta-analysis yielded 279 DEPS. No significant enriched pathways emerged indicating that this approximation was useful to detect the specific pathways related to the protective phenotype.

2.3.3.4 Discussion

The injury by ischemia reperfusión is a common complication of transplantation and vascular disease, the development of strategies able to reduce the damage for this type of acute stress will improve the rate of success of organ transplantation and the survival after a vascular occlusive event. Reduced food intake without malnutrition increases lifespan and acute stress resistance, the best known of the stress-protective dietary interventions is the dietary restriction (DR), it consists in a reduction of the caloric ingest, -typically 30%-. Research had been performed to identify which is the better combination of duration and type of restriction in a diet able to activate the protective response against acute stress (31, 37, 61). It has been shown that two weeks of 30%DR or three days fasting induce a complete protection in a murine renal IRI model (5). It is not realistic for a patient to receive a diet of two weeks of 30%DR and three days fasting could be deleterious for the post-surgery recovery (37). Then is necessary to

identify other dietary regimens able to activate the protective response in a shorter time and without repercussion to the patient outcome.

In this research was demonstrated that protein-free diet for three days is sufficient to induce a complete protection for renal IRI, whereas fat- and carbohydrate-free diets did not. These results incorporate a new dietary protocol that induces the protective response. The emerging questions is whether the molecular pathways responsible for the protection are similar among all the dietary restriction protocols. If this is true, the simultaneous analysis of all responses will be informative about the central pathways responsible for the increases of the stress resistance in those experimental models. Although the mechanism responsible for the increase in life-health span and stress resistance of long-term and short-term DR have been studied intensively, they are still subject of investigation. Various pathways, factors, and genes have been proposed to play a central role in the protective effects (62), but attempts to validate these yielded conflicting results (63-65). The identification of the central pathways related to the protection could orient the development of pharmacological mimetic.

In order to identify a potential transcriptomic signature related to the protective response, gene expression datasets of kidneys from mice exposed to diets proven to be either protective or not protective against renal IRI were generated and analyzed with different bioinformatics strategies. The samples were collected and hybridized in two different batches, one batch was composed by macronutrient deprivations diets and 30%DR, and fasting samples correspond to the other batch. Affymetrix chips and in general transcriptomic technologies are very sensitive to the date of hybridization (66, 67). There are several strategies to correct the batch effect; however, when there is an unbalanced experimental design (there are not samples of all experimental groups in the same batch) the batch correction is not possible. The effect of the batch can be identified using algorithms that reduce the dimensionality; they show in an unbiased way the distribution of the sample. When a principal component analysis (PCA) was performed on all the datasets (Fig 5), the effect of the different dates of hybridization was evident.

The identification of DEG in each individual dietary intervention showed that there is a correlation between the extension of the modification of the transcriptome and the intensity of the restriction. Fasting by three days induced five times more DEG than the other protective diets. Two weeks of dietary restriction had a similar extension of the de-regulation than three days of protein-restricted diet (Table 5). Additionally, the number of DEG after two weeks or three days of 30%DR was similar (492 vs. 391 DEG). Between the other two non-protective diets, CHO-free diets had the second biggest number of DEG in the datasets analyzed (1717 DEG) with almost two times more down-regulated genes than up-regulated genes. Because carbohydrates are the preferred source of fuel, the extensive transcriptional response was expected, the organism should adjust the metabolism to use different sources of energy. While fat-free diets did not induce any detectable modification in gene expression. It agrees with cohort studies in humans reporting that low-fat diets do not have an important impact on health or disease (68-70).

To identify the possible common transcriptional response related to the protective phenotype, with all the list of DEG the overlapping and EF were calculated (Table 6). As a positive evidence of a common response, the EF among all the protective diets were statistically significant and ranging from eight to 22.3. Comparisons including three days fasting had the smaller EF. The EF is sensitive to the size of the lists (71) and fasting by three days induced the wider transcriptional response. In the same direction, fasting had the larger number of DEG in common with other diets, indicating that its transcriptional response included most of the genes

deregulated in the other responses. As an indicator of the complexity and subtlety of the studied phenomena, there were also parallels among protective and non-protective diets. The larger EF were found between the no-protective exposition of 3 days 30%DR and 2 weeks 30%DR and between 3 days 30%DR and 3 days of the protein-free diet. Additionally, CHO-free diet showed a considerable overlap with gene expression profiles of protective diets (Table 6). Those results evidence that there is a transcriptional common response after protective and non-protective dietary modifications under study.

Because fasting results in the wider transcriptional response and it includes more of the DEG as the response of the other diets, we speculated If delimitated the study to only the DEG after fasting could give a better perspective about the relation of the samples from the different dietary interventions. A PCA plot was calculated filtering all the dataset with the DEG after fasting (Fig. 6). Three clusters were evident, the first cluster was on the negative part of PC1; it was composed by control and fat-free diet samples. The protective diets plus three days of 30%DR samples were located in the positive part of both PCs. In addition, a third cluster separated the CHO-free diet samples in the positive part of the PC1 and negative region of PC2. This result finally generates convincing evidence that there is a common transcriptional de-regulation and this response can be differentiated to the response common to protective and non-protective interventions.

Next, a Venn diagram was calculated with the DEG of the protective diets (Fig. 7). The analysis of the intersection of the lists of DEG produces a robust list of DEG (72) but because the statistical power of a microarray study is lower than 50% is also conservative (73). There were 70 DEG in common. This list of genes represent the core of the transcriptional protective response but the number was insufficient to find pathways de-regulated related with the phenotype. A similar analysis with the intersection of de-regulated pathways identified by an over-representation analysis with IPA neither identify relevant biological information (Table 7).

In order to overtake the limitations of the previous analytical approximations, a meta-analysis was performed. Meta-analysis techniques are useful to integrate datasets with the aim to increase the statistical power and to improve the biological interpretation (48). Combining rank orders was used because outliers do not affect it and it produces a robust list of DEG in common (48). The integration of all protective diets identified 640 DEG. Pathways analysis on those genes found well-characterized pathways induced by stress as NRF2-mediated oxidative stress response and glutathione-mediated detoxification. The identification of those pathways indicated that the meta-analysis is able to capture biological meaningful signals. The top up-regulated pathways included the retinoid X receptor (RXR), the farnesoid X receptor (FXR) and the pregnane X receptor (PXR), all of them promiscuous nuclear hormone receptors (48). There are important evidence that the activation of those pathways could be the key process related with the activation of the protective response. The retinoid X receptor is activated by retinoic acids (RAs) (48), administration of RAs induces many of the beneficial effects observed after DR as ameliorate age-related insulin resistance and degenerative brain diseases (74, 75). Additionally, RAs protect from ischemic stroke in the brain (76-78). The FXR activation protects against fatty liver injury, improved hyperlipidemia, glucose intolerance, and insulin sensitivity (79). Finally, the PXR is the major transcriptional regulator of hepatic drug metabolism and protects the vasculature from oxidative stress (79). It is necessary additional experimental evidence to identify the importance of those pathways in the protective response, but the use of synthetic activators of those receptors looks like a promising line of research to development pharmacological activation of the stress resistance

3. CHAPTER 2

TCR-NER deficient mice as model of neurodegenerative disease

3.1 Introduction

Aging significantly affects the central nervous system (CNS); signs of this are the normal cognitive deterioration associated with age and the greater incidence in elderly people of neurodegenerative diseases (ND) such as Alzheimer´s and Parkinson´s disease. Thus, it is not surprising that both people with progeroid syndromes due to TC-NER deficiency (80, 81) as well as mouse models with these syndromes should have phenotypes related to the premature loss of CNS function (19, 82).

The consistent relation between progeroide syndromes and ND plus the fact that neurons are post-mitotic cells, makes plausible the idea that they are particularly sensible to accumulation of DNA damage with age. Additionally, the susceptibility of certain regions of the brain to be target of damage in ND could be related with a differential ability to repair the DNA damage. We hypothesized that there are lower level expression of genes involved in the TC-NER in brain regions typically damage in ND. To gather preliminary insights in this direction, a meta-analysis on datasets from five microarray experiments on human brains available from the open source repository of the Allen Institute for Brain Science (Allen Human Brain Atlas, http://human.brain-map.org/) (82) was performed. The analysis focused on identify in several brain regions the level expression of 38 genes annotated in NER. With this information, a two-way cluster analysis was drawed to facilitate the visualization and identification of specific patterns of gene expression. Areas with a similar pattern of expression of NER genes were grouped together using the Euclidean distance (Fig. 1).

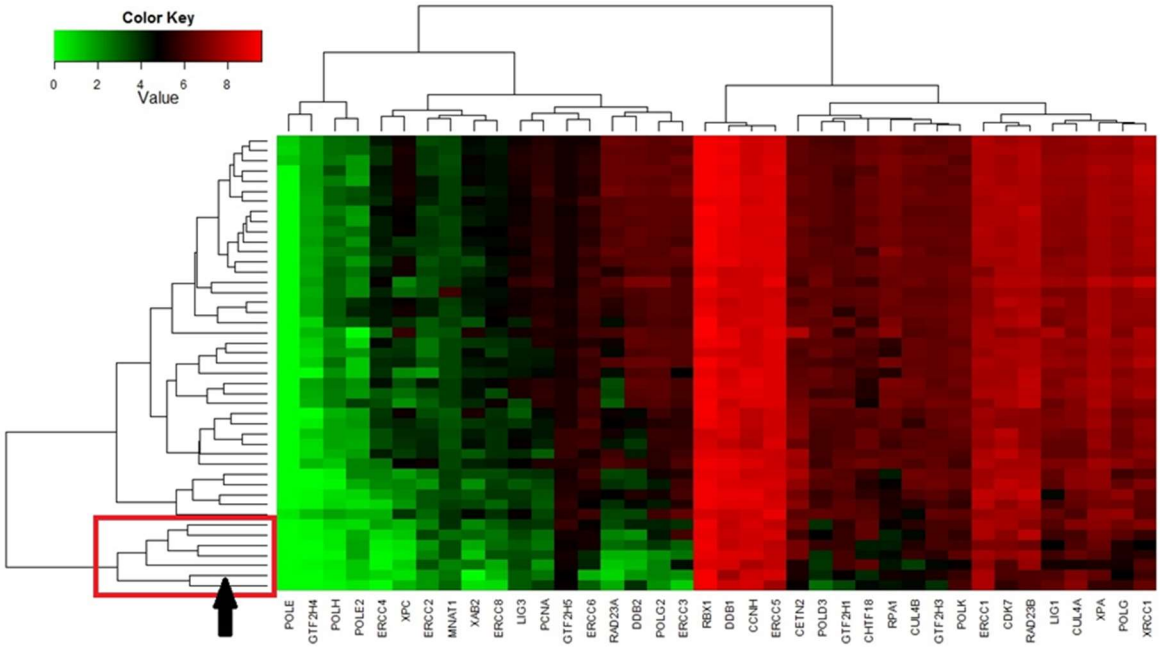

Figure 1. Heat map and two-way cluster analysis of transcription profile of TCR-NER genes in the normal human brain. Genes are on the horizontal axis, brain areas are on the vertical axis. The analyses with a complete review of the relation between TCR-NER and ND were already published (26).

The anatomical areas were ordered into two clusters according to the gene expression levels. Regions involved in the initial stages of ND fall in the low expressing group (Fig. 1, red square in the lower portion, the black arrow pointed the *substantia nigra*). An emerging question of these results was: could the decreased expression of TCR-NER genes result in decreased DNA repair capacity and this could contribute to the selective vulnerability of these cells?

To study the link between DNA damage accumulation and ND, the transcriptome of the *substantia nigra* from mice Ercc1Δ/+ was extensively characterized and compared with molecular signatures of patients with Parkinson disease (PD) and incidental Lewy body (ILBD) disease.

The reasons to use the Ercc1Δ/+ mice as a model was the previous confirmed relation between the Ercc1 deficiency and premature brain damage (26, 27). The most severe deficiency Ercc1-/- mouse (null/null alleles) and the moderate deficiency Ercc1Δ/- mouse (deletion of seven carboxyl terminal amino acids/null allele) show accelerate aging and severe neurological phenotype. Which make impracticable to study the consequences of accumulation of progressive damage in brain. The Ercc1Δ/+ mouse does not have an evident phenotype but is expected to have a lower ability to repair stochastic DNA damage.

Parkinson's disease (PD) was selected as ND model because the *substantia nigra* was identified as one of the critical brain regions with lower expression of TCR-NER. Parkinson's disease is a common neurodegenerative disorder characterized by degeneration of dopaminergic (DA) neurons in the *substantia nigra pars compacta* (SNpc). Incidental Lewy

bodies (ILBD) were also studied because the actual state of knowledge points that they may represent preclinical PD (83).

This research was performed in parallel with an extensive cellular, molecular and neurological characterization of the phenotype of the Ercc1Δ/+ mice. The multidisciplinary team of researchers that performed the experiments was under the direction of professor Pier Mastroberardino at Erasmus MC. This chapter is an adaptation of a paper already published with the results of this research (84).

3.2 Methods

3.2.1. Animals

Generation and characterization of NER mutants Ercc1Δ/+ mice has been previously described (85). Ercc1Δ/+ mice were generated in a FVB:C57BL/6J (50:50) genetic background. Animals were kept on a regular diet and housed at the Animal Resource Center (Erasmus University Medical Center). It operates in compliance with the “Animal Welfare Act” of the Dutch government.

3.2.2. RNA seq

For RNA extraction four Ercc1Δ/+ and four wt mice 52 weeks old were killed by cervical dislocation, brains were rapidly excised on an ice-cold plate. Total RNA was isolated from the ventral mesencephalic area of the mouse brain using the RNAqueous Kit (Ambion) according to manufactures directions. Briefly, ventral midbrain tissues were homogenized in RNA lysis buffer and stored at -80^C until the extraction procedure. RNA quality was assessed via the BioAnalyzer machine (Agilent 2100).

3.2.3. mRNASeq sample preparation

Total RNA enrichment for sequencing poly(A) RNAs was performed with the TruSeq mRNA sample preparation kit (Illumina) according to the manufacturer’s protocols. In short, 1 μg of total RNA for each sample was used for poly(A) RNA selection using magnetic beads coated with poly-dT, followed by thermal fragmentation. The fragmented poly(A) RNA enriched samples were subjected to cDNA synthesis using Illumina TruSeq preperation kit according to the manufacturer’s protocol. Briefly, cDNA was synthesized by reverse transcriptase (Super-Script II) using poly-dT and random hexamer primers. The cDNA fragments were then blunt-ended through an end-repair reaction, followed by dA-tailing. Subsequently, specific double-stranded bar-coded adapters were ligated and library amplification for 15 cycles was performed.

3.2.4 Sequencing

Pooled cDNA libraries all consisted of equal concentration bar-coded samples (wt and Ercc1d/+ samples) were sequenced in one lane each on the HiSeq2000 (Illumina).

3.2.5 mRNASeq analysis

Reads were aligned to the mouse mm9 reference genome using Tophat (version 1.3.1.Linux_x86_64, --coverage-search, -butterfly-search, --segment-mismatches 1,--segment-length 18) via the NARWHAL automation software (86).

SAMMate (http://sammate.sourceforge.net/) (87) was used to detect and quantify transcripts. Gene counts were calculated taking into account the reads mapped on exons or on exon-exon junctions.

Differentially expressed genes were detected using the R package EdgeR (PMID: 24743990). It is a Bioconductor software package for examining differential expression of replicated count data. To account for biological and technical variability an overdispersed Poisson model is used. The degree of overdispersion across transcripts is moderate with an Empirical Bayes method. Genes with a false discovery rate (FDR) of < 0.05 and fold change ±1.5 were considered to be differentially expressed.

3.2.6 Human Parkinson and incidental Lewy body datasets analysis

Microarray data from human substantia nigra were obtained from GEO Omnibus repository (http://www.ncbi.nlm.nih.gov/geo/). Three subseries from superserie GSE20186 (88) were used in this analysis. Subserie GSE20159 consists of snap-frozen humain *substantia nigras* of 16 individuals with a clinicopathological diagnosis of incidental Lewy body (ILBD) disease. Subserie GSE20163 consists of SNs samples from 8 PD subjects obtained from the Human Brain and Spinal Fluid Resource Center, VAMC, and 9 control subjects obtained from the University of Rochester Alzheimer's Disease Center brain bank. Subseries GSE20164 consists of SNs samples from 6 PD and 5 control subjects obtained at autopsy, brain hemispheres were frozen in liquid nitrogen and stored at -80C in the Kathleen Price Bryan Brain Bank in the Alzheimer's Disease Research Center at Duke University.

Samples in subserie GSE20159 were hybridized in Illumina HumanHT-12v3 Expression BeadChips, this data was already normalized in GEO database by average normalization and under quality-control using GenomeStudio. Differences between samples from ILBD compared with samples from normal controls were calculated with the tool GEO2R that uses the linear model for microarray data analysis (Limma) package implemented in R.

Samples in subseries GSE20163 and GSE20164 were hybridized in Affymetrix Human Genome U133A Array. They were normalized by robust multichip average (RMA) in the oligo BioConductor package, which normalizes the intensity values at the transcript level and collapses probes into core transcripts based on annotations provided by Affymetrix. Because the samples sizes of both subseries were small, they were combined in one bigger dataset. The non-biological variation and batch effects were adjusted using a nonparametric empirical Bayes methodology as it is implemented in Combat (PMID: 16632515). Limma was used to calculated fold changes and p values on pairwise comparisons between Parkinson samples and control samples.

3.2.7 Pathway analysis:

Pathway enrichment analysis was conducted via two different approaches: Overrepresentation analysis (ORA) and Gene set enrichment analysis (GSEA).

ORA was performed in the Interactive pathway analysis (IPA) of complex genomics data software (Ingenuity Systems, www.ingenuity.com, Redwood City, CA) by employed a pre-filtered list of differentially expressed genes. The overrepresented canonical pathways were generated based on information in the Ingenuity Pathways Knowledge Base. A Fisher exact test was performed to determine the likelihood of obtaining at least the equivalent numbers

of genes by as actually overlap between the input gene set and the genes present in each identified pathway.

GSEA was conducted on an unfiltered ranked list of genes. Genes in each dataset were ranked by the level of differential expression using a combination of Log2Fold change and the p-value as was proposed by Xiao (89).

$$\pi_i = \frac{|Fc_i|}{Fc_i} pi^{Fc_i}$$

Where:

Πi = Modified pvalue of gene i

Fci = Log2 fold change of gene i

pi = pvalue of gene i

Statistical significance of pathway enrichment score was ascertained by permutation testing over size-matched random gene sets, and multiple testing was controlled by false positives a family-wise error rate (FWER) threshold of 5% was used (90), this statistical is more conservative than FDR. Pathway information was collected from Kyoto Encyclopedia of Genes and Genomes (KEGG) available at the Molecular Signatures Database (http://www.broadinstitute.org/gsea/msigdb/index.jsp). Because pathway in KEGG are redundant (two o more pathways shared more than 75% of the genes), the R package Recipa (91) was used to reduce the redundancy among KEGG pathways. Pathways with an overlapping higher than 75% in their genes were collapsed in one.

3.2.8 Comparison among transcriptomes of Ercc1Δ/+, PD and ILBD datasets:

In this research were used four datasets from two different organisms (human and mouse) and from three different platforms (Rna-Seq, Illumina and Affimetrix). Then to do a fair comparison among them, the genes in each platform where filtered to do the comparison analysis with common genes across the studies.

The final lists of deregulated pathways were compared by a counting method (Venn diagram). To determinate if the overlapping were higher than expected by chance a hypergeometric distribution was used. Additionally the factor of enrichment was calculated with the formula:

EF=nAB/((nA×nB)/nC)

Where:

nA = Number of deregulated pathways in dataset A
nB= Number of deregulated pathways in dataset B
nC= Number of total pathways in KEGG database
nAB = Number of common deregulated pathways between A and B

3.3 Results:

3.3.1. Characterization of the transcriptome of *substantia nigra* from Ercc1 Δ/+ mice.

Comparison of the RNA-seq of four samples of *substantia nigra* from Ercc1 Δ/+ 52 weeks old with the transcriptome of four wt samples matched by age revealed 460 differentially expressed genes (DEGs), 187 of which were up- and 273 down-regulated.

Biological interpretation of the differential profiles were determined using overrepresentation analysis (ORA) to highlight significantly altered specific functional categories. Modified pathways included relevant processes for PD, including oxidative phosphorylation, mitochondrial dysfunction, and proteasome. Interestingly, EIF2-signaling pathway, which constitutes the pathway with highest significance in the analysis (Table 1), has been linked as potential biomarker in both genetic and sporadic forms of the disease (92). These results support the concept that inefficient TCR-NER affects biological processes relevant for the dopaminergic system integrity and their possible relation to the development of ND.

Ercc1d vs wt Ingenuity Canonical Pathways	P-value
EIF2 Signaling	0
Oxidative Phosphorylation	0
Mitochondrial Dysfunction	0
Huntington's Disease Signaling	0
Calcium Signaling	0.0002
Role of NFAT in Cardiac Hypertrophy	0.0002
Sperm Motility	0.0003
Dopamine-DARPP32 Feedback in cAMP Signaling	0.0004
Glutamate Receptor Signaling	0.0004
G-Protein Coupled Receptor Signaling	0.0005
Neuropathic Pain Signaling In Dorsal Horn Neurons	0.0007
Chemokine Signaling	0.0009
Protein Kinase A Signaling	0.0009
mTOR Signaling	0.0011
Regulation of eIF4 and p70S6K Signaling	0.0011
Gαq Signaling	0.0011
Aldosterone Signaling in Epithelial Cells	0.0014
CCR3 Signaling in Eosinophils	0.0015
nNOS Signaling in Neurons	0.0016
Synaptic Long Term Potentiation	0.0019

Table 1. Top 20 de-regulated pathways in substantia nigra in Ercc1Δ/+ mice. Over-representation analysis was performed with IPA. The directionality in the change of the pathways is not provided because up- and down-regulated genes were analyzed in one batch.

3.3,2 Identification of parallels and divergences among transcriptomic of *substancia nigra* of Ercc1Δ/+ mice and from patients with PD and ILBD.

To identify whether the transcriptomic de-regulation in Ercc1Δ/+ mice recapitulated human pathology a pathway comparative analysis was performed. The ranking algorithm implemented in Gene set enrichment analysis (GSEA) was used on gene collections as defined by the Kyoto Encyclopedia of Genes and Genomes (KEGG) with a previously reduced redundancy. GSEA was used because it is designed to detect modest changes in the expression of groups of functionally related genes (93). Parkinson and ILBD are complex phenotypes and the heterogeneity of the human population is high then it is necessary to use a sensible technique to identify de-regulated pathways. Additionally, datasets involved in the comparison had different transcriptomic techniques and ranking method increases the comparability among heterogeneous datasets (94). The comparability of the results of GSEA (Table 2) with the over-representation analysis is restrained because in both analysis different set of pathways were used. However, the biological meaning of the de-pathways shows large similarities.

A.

Up-regulated

NAME	FDR q-val
KEGG_FOCAL_ADHESION_+_KEGG_ECM_RECEPTOR_INTERACTION	0
KEGG_MAPK_SIGNALING_PATHWAY	0
KEGG_REGULATION_OF_ACTIN_CYTOSKELETON	0
KEGG_PATHWAYS_IN_CANCER	0
KEGG_JAK_STAT_SIGNALING_PATHWAY	0
KEGG_AXON_GUIDANCE	3.60E-04
KEGG_PHOSPHATIDYLINOSITOL_SIGNALING_SYSTEM_+_KEGG_INOSITOL_PHOSPHATE_METABOLISM	4.05E-04
KEGG_CALCIUM_SIGNALING_PATHWAY	4.17E-04
KEGG_FC_GAMMA_R_MEDIATED_PHAGOCYTOSIS	4.28E-04
KEGG_GNRH_SIGNALING_PATHWAY	4.52E-04
KEGG_INSULIN_SIGNALING_PATHWAY	4.62E-04
KEGG_CYTOKINE_CYTOKINE_RECEPTOR_INTERACTION	4.93E-04
KEGG_VEGF_SIGNALING_PATHWAY	5.40E-04
KEGG_TYPE_II_DIABETES_MELLITUS	5.56E-04
KEGG_DILATED_CARDIOMYOPATHY_+_KEGG_HYPERTROPHIC_CARDIOMYOPATHY_HCM	6.79E-04
KEGG_NEUROTROPHIN_SIGNALING_PATHWAY	7.82E-04
KEGG_TGF_BETA_SIGNALING_PATHWAY	0.0026

B.

Down-regulated

NAME	FDR q-val
KEGG_RIBOSOME	0
KEGG_OXIDATIVE_PHOSPHORYLATION	0
KEGG_HUNTINGTONS_DISEASE_+_KEGG_PARKINSONS_DISEASE	0
KEGG_ALZHEIMERS_DISEASE	0
KEGG_PROTEASOME	0
KEGG_PYRIMIDINE_METABOLISM	0
KEGG_PEROXISOME	1.19E-04
KEGG_GLUTATHIONE_METABOLISM	1.95E-04
KEGG_SYSTEMIC_LUPUS_ERYTHEMATOSUS	2.66E-04
KEGG_VALINE_LEUCINE_AND_ISOLEUCINE_DEGRADATION	7.51E-04
KEGG_DRUG_METABOLISM_CYTOCHROME_P450_+_KEGG_METABOLISM_OF_XENOBIOTICS_BY_CYTOCHROME_P450	0.0024
KEGG_PURINE_METABOLISM_+_KEGG_RNA_POLYMERASE	0.0024

Table 2. Up- and Down-regulated pathways in *substantia nigra* from Ercc1Δ/+ as was established by GSEA. The GSEA was performed on the KEGG pathways database with a previous processing oriented to collapse pathways with more than 75% of genes in common. The collapsed pathways are represented with a "+" symbol.

The GSEA were performed on publicly available datasets from human PD and ILBD, which is regarded as a pre-symptomatic form of PD (83) and the discovered pathways were compared with the Ercc1Δ/+ de-regulate pathways. Of the 12 pathways down-regulated in Ercc1Δ/+ (Table 2B), five were shared with ILBD and/or PD and include relevant processes for PD, such as oxidative phosphorylation, glutathione metabolism, proteasome (Fig. 2 and 3). The gene set KEGG_PARKINSONS_DISEASE (http://www.broadinstitute.org), which was consolidated with the KEGG_HUNTINGTONS_DISEASE pathway after redundancy reduction, is down-regulated in all datasets, further demonstrating affinities between the mouse model and the human disease. Of the 17 up-regulated pathways in Ercc1Δ/+, seven were shared with PD and none with ILBD (Fig. 2 and 3). Common up-regulated pathways include inflammation and mitogen-activated protein kinase (MAPK) signaling, which are both relevant for human PD (PMID: 23665870, PMID: 21395478). In summary, transcriptomic analyses highlight important molecular similarities between Ercc1Δ/+ mice and the human disease.

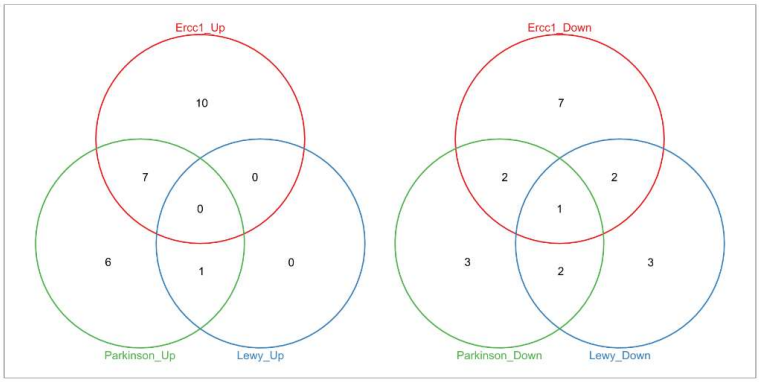

Figure 2. Venn diagram showing the intersection of de-regulates pathways in substantia nigra of Ercc1Δ/+ and patients with PD and ILBD. Adapted from (84)

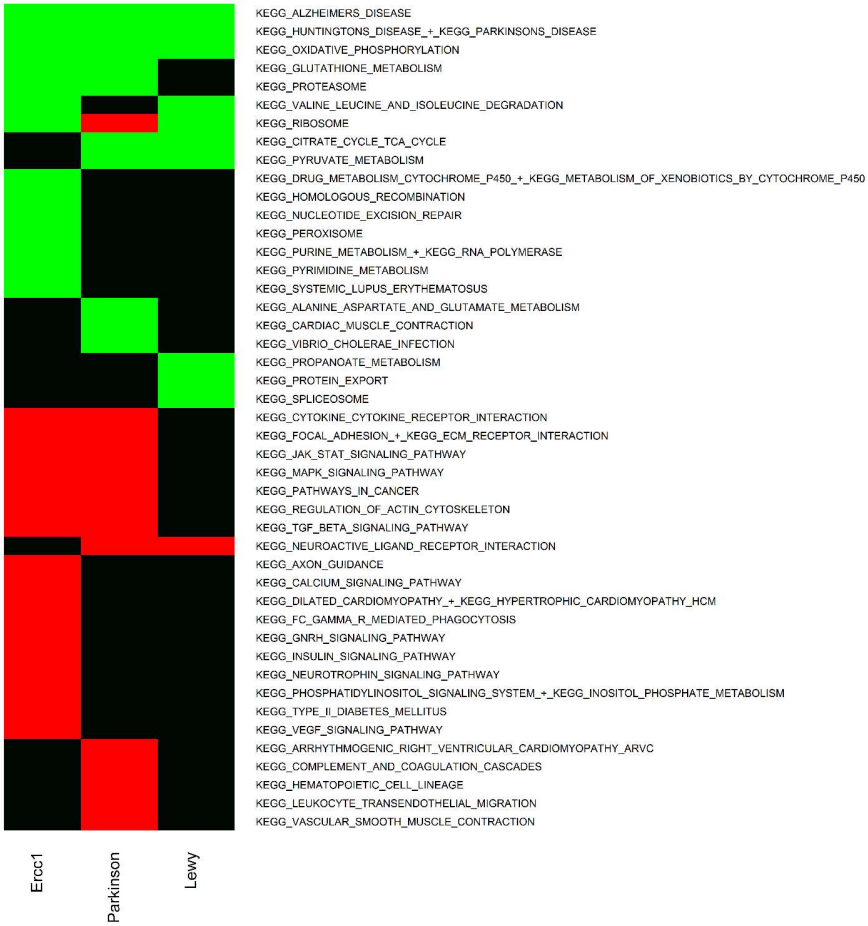

Figure 3. Heatmap showing the common de-regulated pathways in Ercc1Δ/+ mice, in PD, and in ILBD. Red means up-regulation, green means down-regulation, black means do not change**.** Adapted from (84)

Enrichment factors calculation (EF) was used to determinate objectively the strength of overlapping between Ercc1Δ/+ and human PD and ILBD. EF estimates similarity between datasets by comparing the extent of abundance of common elements in the groups under consideration (e.g., Ercc1Δ/+ and PD) with the extent of abundance that would be expected in random groups.

	All		Up		Down	
Comparison	**EF**	**p value**	**EF**	**p value**	**EF**	**p value**
Ercc1 ∩ Parkinson	1.2	2.53E-01	2	4.23E-02	6.7	8.82E-05
Ercc1 ∩ Lewy	0.7	9.61E-01	0.5	9.25E-01	5.6	1.77E-05
Parkinson ∩ Lewy	2.8	1.79E-07	9.2	1.80E-05	4.2	6.51E-08

Table 3. Enrichment factor and p values of the overlapping. Enrichment factor means how many times there are more or less pathways in common than expected by chance. Adapted from (84)

The number of common down-regulated pathways in related pathologies such as PD and ILBD is 4.2 times more abundant than what expected by chance ($p < 10^{-7}$; Table 3). Down-regulated pathways common to Ercc1Δ/+ and PD and to Ercc1Δ/+ and ILBD are, respectively, 6.7 and 5.6 more abundant than what would be expected by chance ($p < 10^{-4}$). There was not a significant enrichment in up-regulated processes shared between Ercc1Δ/+ and ILBD, whereas there was a 2-fold enrichment ($p < 0.0005$) when comparing Ercc1Δ/+ and PD. As expected, the number of common up-regulated pathways between both PD and ILBD human datasets was 9.2 times more abundant than what would be expected by chance ($p < 10^{-4}$). These additional analyses further confirm affinities between the transcriptional landscape of Ercc1Δ/+ and human PD with stronger similarity on down-regulated pathways.

3.4 Discussion

Here is presented evidence that the transcriptome of *substantia nigra* in Ercc1 Δ/+ mice 52 weeks old shows striking similarities with the transcriptome of patients with PD and moderate parallels with the transcriptome of patients with ILBD.

The complete phenotypical characterization of Ercc1 Δ/+ mice support the RNA-seq conclusions (or vice versa). The mice with the slight deficiency in TCR-NER share with patients with PD, pathological alterations in DA neurons, as increased in the level of oxidation, more γH2AX foci, defects in protein homeostasis, impairment of proteosomal activity, higher levels of phosphorylated α-syn (p129S) and increases astrocyte activation in the *substantia nigra*. The recapitulation of the PD phenotype is extended also to the mitochondrial function. Mitochondrial C-I defects are relevant in the pathology of PD, Ercc1Δ/+ mice had a decreased basal (i.e., state 2 = state 4) and ADP-stimulated (i.e., state 3) respiration in cells from the ventral mesencephalon (84).

The ND in Ercc1 Δ/+ mice compatible with several characteristics of PD pointed the importance of NER in non-dividing neurons. A study exploring differentiated neurons and their precursors (PMID: 10669734), demonstrated that specialization induces up-regulation of the two NER specific nucleases XPG and XPF/Ercc1, thus indicating that those genes may be particularly relevant for mature neurons. Additionally, recent research described the relevant role of DNA damage and repair in the physiopathology of PD. Synucleinopathy models of Parkinson's disease showed activation of the DNA damage response in vivo probably mediated by oxidative stress and mitochondrial dysfunction (95).

The comparison of down-regulated pathways showed significant EF among Ercc1 Δ/+ with both PD (EF 6.7) and ILBD (5.6). The EF between PD and ILBD was 4.2, that indicates that Ercc1 Δ/+ resembles better the PD down-regulated transcriptome that a less severe state of the disease. Conversely the up-regulated pathways showed more resemble between PD and ILBD (EF 9.2) compared with Ercc1 Δ/+ and PD (EF 2). This discordance between the overlapping depending of the direction of the de-regulation could be in agreement with the type of damage that is accumulated with the deficient of TCR-NER. The TCR-NER is responsible to repair de DNA damage in transcriptionally active genes, the accumulation of this type of damage produce a passive down-regulation of gene expression. In Ercc1 -/- mice, with a severe progeroid phenotype was found a preferential down-regulation of longest genes (96). The pathways up-regulated only in PD are pathways related with inflammation as leukocyte trans endothelial migration, or vascular function as complement and coagulation cascades, hematopoietic cell linage and vascular smooth muscle contraction. Because PD is a multifactorial disease where genetic-environmental interactions are fundamental is possible that in Ercc1 Δ/+ there is the expression of the genetic factors but because there are growing in controlled conditions the absence of the exposition of environmental factor restrict the activation of the other part of the pathological response as inflammatory pathways.

In conclusion, the research provide novel evidence proving that inefficient NER could be at least a modification in idiopathic and genetic PD patients; and describe a new potential model of sporadic PD.

4. CHAPTER 3

Integrative analysis of global gene expression identifies opposite patterns of reactive astrogliosis in aged human prefrontal cortex

4.1 Introduction

Aging is the physiological and morphological decline of individuals with the passing of time, which increases their susceptibility to diseases such as cancer, diabetes, neurodegenerative and cardiovascular disorders, and ultimately increases their vulnerability to death. It has become a public health problem since life expectancy has increased, with a consequent world population aging (8).

The brain undergoes functional alterations during aging. The age-related changes do not show a unique pattern across different individuals (97). At the same age, some people exhibit characteristics of a healthy aging, but others manifest diminishing motor, sensory and cognitive abilities, in addition to increased risk of suffering neurodegenerative and neuropsychiatric diseases. The prefrontal cortex (PFC) seems to be morphological and functionally more vulnerable to the effects of aging compared with others areas (98). Molecular and cellular responses to aging have been described, for example, neurons show deregulation of transmission, formation, and elimination of synapses. In astrocytes has been reported an increase of the activation with aging. Recently was identified up-regulation of genes of reactive astrocytes that are induced by neuroinflammation in brain mouse (99). However, the complete molecular mechanisms related to normal human brain aging are not completely understood.

Transcriptomic studies have been successful to identify some of the specific processes described before (100) (101) (102) (103). However, they have limitations, main restrictions of those kinds of analysis is the inter-individual variability of the aging process, the complexity of getting samples from human's brains and the intrinsical technical variation of the transcriptomic methodologies. We hypothesize that combining independent studies by meta-analysis could help us to identify the central and common process associated with PFC aging avoiding the non-general process specific of a particular dataset.

We combined by meta-analysis the PFC gene expression profile from two different age groups - 58-80 years and 20-40 years- from four independent studies. We selected those range of ages given that until the forties it had been described that genes expression maintain a homogeneous pattern with a low rate of change, and after this period, the changes begin to rise through several decades to become homogeneous again around sixties. Bioinformatics analysis of the result of the meta-analysis suggests that in older individuals the neuronal activity declines without necessarily presenting cell death or massive neuron dysfunction. Clusters of genes with pre-synaptic and post-synaptic functions are down-regulated and over-represented, especially for glutamate, and gamma-aminobutyric acid (GABA) neurons. Additionally, the signature analysis identified the presence of reactive astrocytes in aged PFC. This astrogliosis is characterized by the presence of up-regulation of genes specific for two different types of

reactive astrocytes: A1 and A2. Neurotoxic A-like 1astrocytes were recently described in the brain of old rats (99). But, this is the first time, in our knowledge, that molecular signature of neuroprotective A2 astrocytes are identified in aging of the human PFC.

4.2 Methods

4.2.1 Data Selection

We performed an advanced search in the National Center for Biotechnology Information (NCBI) GEO database (http://www.ncbi.nlm.nih.gov/geo/) to identify studies analyzing global gene expression in the human prefrontal cortex. The advanced search tool was used with the keyword PFC (prefrontal cortex) and studies were limited to *Homo sapiens* as the organism and expression profiling by array as the dataset type. We included studies which met the following conditions: (1) it was performed using any version of Affymetrix chips, (2) studies analyzed at least three samples in each age group (old: 58-80 years old, young: 20-40 years old), (3) the raw data were available, and (4) they passed quality control. We excluded one RNA-Seq study because we wanted to maintain a platform-controlled heterogeneity. The squematic overview of search strategy and selected entries is presented in the Figure 1. and the characteristics of the included studies are shown in the Table 1.

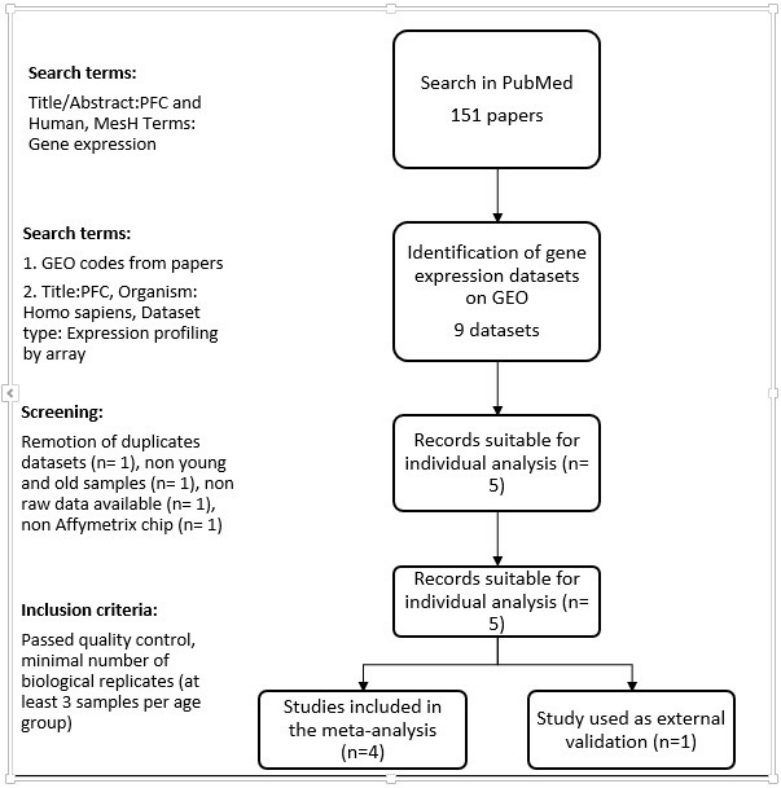

Figure 1. Workflow of the data selection. Search in PubMed and GEO database identified nine datasets involving transcriptomic analysis of PFC in humans. After remotion of duplicates and quality control, five datasets were selected in this research.

GEO code	Brain region	Samples (Old/Young)	Platform	Reference
GSE53987	Pre-frontal cortex	4/4	Affymetrix Human Genome U133 Plus 2.0 Array	PMID: 25786133
GSE11512	Dorsolateral prefrontal cortex	4/8	Affymetrix Human Genome U133 Plus 2.0 Array	PMID: 19307592
GSE17612	Brodmann area 10: anterior prefrontal cortex	7/3	Affymetrix Human Genome U133 Plus 2.0 Array	PMID: 19255580
GSE17757	Superior frontal gyrus region of the prefrontal cortex	4/3	Affymetrix Human Gene 1.0 ST Array	PMID: 20647238
GSE71620	Brodmann area 11	48/39	Affymetrix Human Gene 1.1 ST Array	PMID: 26699485

Table 1. Description of studies included in the analysis. GEO: Gene Expression Omnibus; Young are samples from people between 20-40 years old, Old are samples from people from 58-80 years old. GSE71620 was used as an external validation dataset.

4.2.2 Quality control, batch effect adjustment and data preprocessing

All datasets underwent quality control (QC) using the QC module from ArrayAnalysis.org (104) to evaluate each microarray. Several parameters were used to detect low-quality samples, as a virtual reconstruction of the image, the signal comparability and array correlation. Low-quality microarrays were eliminated for the subsequent analysis.

Data preprocessing was performed using limma R/Bioconductor software package (105). The probesets were summarized, and the data were normalized and then log 2 transformed using the RMA algorithm. Since Affymetrix chips have several probes for the same gene, the most informative probe (that one showing the highest variability across the experimental groups) was kept and the others were discarded.

In order to improve the statistical power and comparability of samples from the same dataset, a batch effect correction was performed using empirical Bayes methods implemented with ComBat (106).

4.2.3 Data integration by meta-analysis

Datasets selected for integration had a similar experimental design, sample size, and chemistry. These datasets were then merged using a modified Fisher's combined p-value meta-analysis implemented through MetaDE R package (107), as was described by Rhodes et al. (108). For each gene in every dataset, a p-value was determined by a t-test, after a p value modified (Pmod) was calculated by multiplying the -log10 (p-value) times log1.5 (absolute fold change). Xiao et al. (89) described in detail the p-value modification using this methodology. This modification allows the p-value to be enriched with the FC magnitude and provides better control of false positives. The Pmods of each gene in all datasets were combined using the Rhodes methodology.

4.2.4 Biological interpretation

DAVID (https://david.ncifcrf.gov/) was used to identify the functions of the selected differentially expressed genes (DEG). The Kyoto Encyclopedia of Genes and Genomes (KEGG) and gene ontology biological function pathways databases were chosen for the over-representation analysis. Pathways with p-values lower than 0.05 were selected as enriched.

4.2.5 Signature analysis

Over-representation and under-representation analysis were performed using the hypergeometric test as is implemented in the over-representation enrichment analysis described in WebGestalt (109). Molecular signatures of specific cells, region of cells or molecular phenotypes were mined from the public literature. Signatures were interrogated against lists of DEG in order to identify if there are more (over-representation) or fewer (under-representation) genes from the signature in the DEG than expected by chance.

4.3. Results

4.3.1 Data selection

After the PubMed and GEO omnibus database search, five studies met the inclusion criteria (Fig. 1): GSE53987 (110), GSE11512 (111), GSE17612 (112), GSE17757 (113) and GSE71620 (100). All selected studies were performed using the Affymetrix platform, in humans, with at least three biological replicates for each experimental group (old, young) and they were from different regions of the PFC (Table 1). The first four studies were used to perform the meta-analysis and the last one was used for external validation of the meta-analysis. GSE71620 was selected as validation study because it had a large number of biological replicates. We considered that results obtained by the integrative analysis of several small and independent studies which are concordant with the one single big study, implies that the conclusions of the integrative analysis are robust.

4.3.2 Quality control, batch effect adjustment and data preprocessing

All arrays involved in the analysis were evaluated for the quality of several parameters (Fig. 2). The data quality was determined through RNA degradation ratios, relative log expression and normalized unscaled standard errors using the Arrayanalysis.org platform (104). Low-quality arrays were removed and the complete datasets were analyzed again to reassess the quality of the remaining samples.

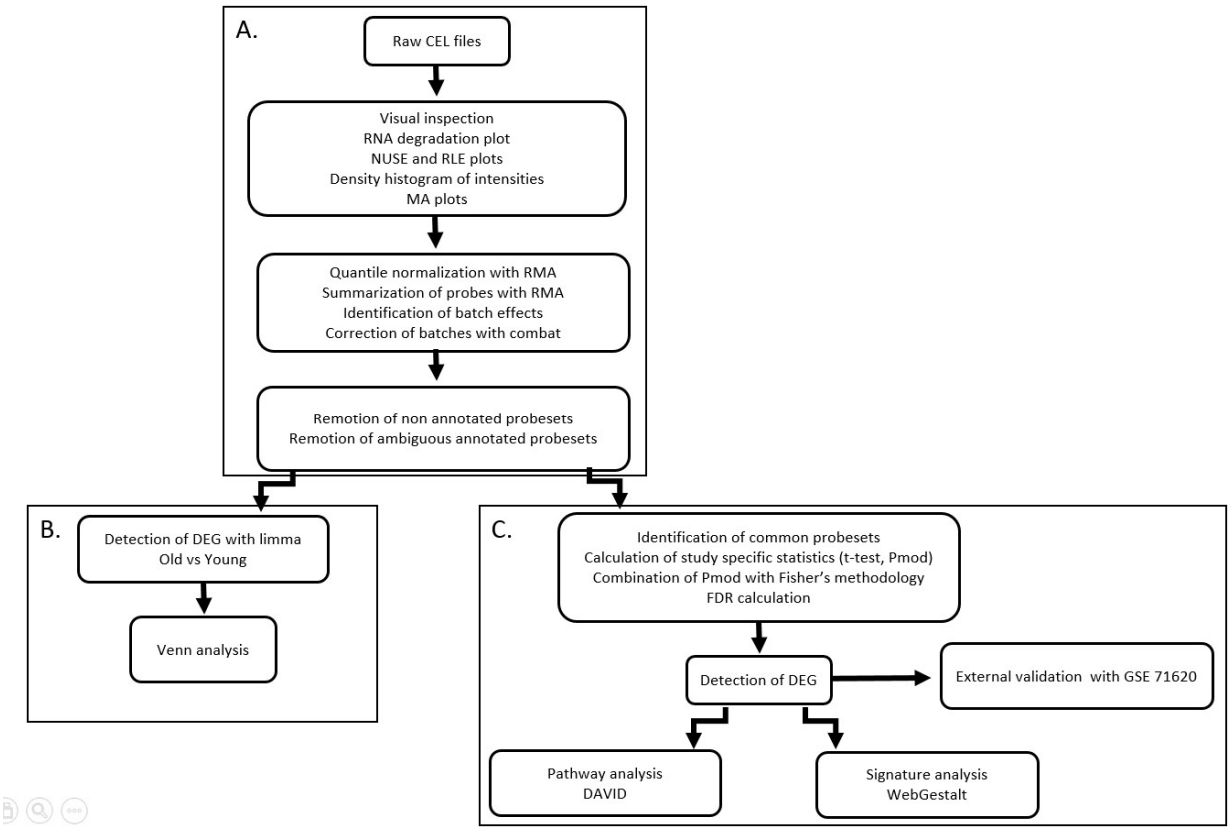

Figure 2. Study workflow. Study was performed in three connected modules. (A)Quality control and preprocessing of individual studies. (B) Each dataset was analyzed individually using limma Lists of DEG were compared by Venn analysis. (C) Datasets were combined by meta-analysis. The DEG were analyzed by pathway over-representation with DAVID and signature analysis was performed using the WebGestalt algorithms. Results of the meta-analysis were validated by comparison with an external dataset (GSE71620)

Following this process, a principal component analysis (PCA) plot was calculated for each dataset in order to detect outliers and to identify the unbiased distribution of the samples. Additionally, the scanning date was identified to detect batch effects. A batch correction was performed using ComBat. After batch correction, PCA plots were recalculated to check the modification in the distribution of the samples. All datasets had batch effects and all datasets were batch corrected. Two samples were removed from GSE71620 because there were outliers, Table 1 summarize the studies and samples after the mentioned processes.

4.3.3 Data integration: meta-analysis of gene expression in old vs. young PFC

The meta-analysis methodology used in the integration of the four studies was designed to increase the statistical power of the individual datasets and provided a strong list of DEG consistently de-regulated across all the comparisons (114). In order to determine how the meta-analysis was able to identify genes that were not recognized by the individual datasets, and to spot the number of genes that were not consistently differentially expressed across the individual analyses, a Venn diagram with the DEG from each individual analysis and from the meta-analysis was calculated using InteractiVenn (115). Figure 3 shows the DEG in each individual analysis compared with the DEG after the meta-analysis. The meta-analysis identified

most of the genes in each individual analysis and was able to detect 598 additional genes. Given that the meta-analysis combined the magnitude of the change in expression, the direction of the change and the level of statistical significance, the detected DEG had the same direction of change across all the datasets in the analysis. A complete list of DEG is presented in Table S1. When the DEG were divided into down-regulated and up-regulated genes (Table 2), down-regulated genes outnumbered the up-regulated ones in a ratio of 2.2:1.

A.

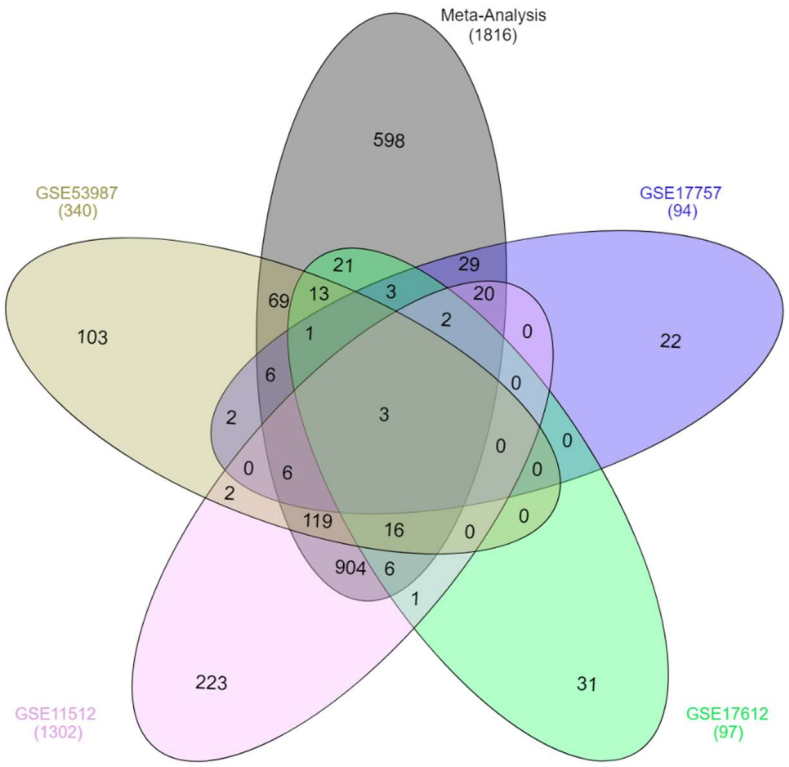

B.

Study	DEG	In Meta-analysis	Proportion	Out Meta-analysis	Proportion
GSE53987	341	238	0.70	103	0.30
GSE11512	1302	1079	0.83	223	0.17
GSE17612	97	66	0.68	31	0.32
GSE17757	94	72	0.77	22	0.23

Figure 3. A) Venn diagram of DEG identified from the individual analysis (GSE11512, GSE17612, GSE53987, GSE17757) and from the meta-analysis. The meta-analysis identified 1218 genes that were identified by the individual analysis (intersection of the black ellipse with others four ellipses) and 598 additional genes that were not identified in any individual analysis. **B)** Number and proportion of DEG from individual analysis and detected by the meta-analysis. In Meta-analysis means the DEG of individual analysis that were preserved in the meta-analysis, Out Meta-analysis means the DEG from individual analysis that were not present in the meta-analysis.

	Meta-analysis	GSE71620	Common genes	Proportion of common genes
DEG	1816	5120	1141	0.63
Up-regulated	561	2076	339	0.60
Down-regulated	1256	3044	783	0.62
Total genes	6895	18989	6895	

Table 2. Summary of number and direction of the change of DEG detected in the analysis. Up-regulated genes are genes with an increase in the expression in old samples compared with young samples and down-regulated genes are genes with lower expression in old samples compared with young samples. Total genes represent the number of genes in each analysis. Common genes are the genes identified simultaneously in both analyses (Meta-analysis and GSE71620). The proportion of common genes are the proportion of genes in common between the meta-analysis and the validation dataset (GSE71620). Those genes had the same direction of change.

The external validation dataset, GSE71620, was analyzed individually with limma: 48 samples from people between 60 to 80 years old were compared with 39 young samples (people from 20 to 40 years old) to detect the DEG (Table S2). Out of a total of 18,989 genes, 5,120 (27%) had an FDR lower than 0.05. Similar to the meta-analysis findings, there were more down-regulated genes than up-regulated genes (1.5:1). In order to have evidence of the reproducibility of the results of the meta-analysis, both lists of DEG were compared (Table 2). More than 60% of the DEG were shared between the meta-analysis and GSE71620, and the majority of them had the same direction of change with aging. Only 19 of 1.141 DEG (2%) had an opposite direction of change. That constitutes a very good overlapping between both analyses, as it is usual to find a very small proportion of common DEG (lower than 10%) when different datasets are analyzed in an independent way (53).

4.3.4 Functional analysis of old PFC

To identify the biological functions of the selected DEG in the meta-analysis, we performed a pathway analysis in DAVID using KEGG and Gene Ontology Biological process (GOBP) pathways databases. Pathways in KEGG and GOBP have several genes in common. Following this, we used the DAVID cluster tool to identify a set of non-overlapping pathways over-represented in the list of DEG. In order to have a better comprehension of the involvement of the pathways in PFC aging, we performed independent analyses with both up-regulated and down-regulated genes. Table 3 shows the pathways over-represented in the down-regulated genes and Table 4 shows the pathways over-represented in the up-regulated genes. Tables S3, S4 presents the list of all genes identified in each pathway.

Cluster 1

Category	Term	Count	FE	PValue
KEGG_PATHWAY	Glutamatergic synapse	34	4.1	1.34E-12
KEGG_PATHWAY	Dopaminergic synapse	34	3.7	4.41E-11
KEGG_PATHWAY	Circadian entrainment	28	4.1	2.48E-10
KEGG_PATHWAY	GABAergic synapse	26	4.3	5.21E-10
KEGG_PATHWAY	Cholinergic synapse	24	3.0	2.78E-06
KEGG_PATHWAY	Serotonergic synapse	22	2.8	3.25E-05

Cluster 2

Category	Term	Count	FE	PValue
GO_BP	potassium ion transmembrane transport	19	2.4	9.52E-04

Cluster 3

Category	Term	Count	FE	PValue
KEGG_PATHWAY	Circadian entrainment	28	4.1	2.48E-10
KEGG_PATHWAY	Oxytocin signaling pathway	26	2.3	1.34E-04
KEGG_PATHWAY	cGMP-PKG signaling pathway	25	2.1	7.13E-04
KEGG_PATHWAY	Long-term depression	13	3.0	9.54E-04
KEGG_PATHWAY	Gap junction	16	2.5	0.001
KEGG_PATHWAY	Inflammatory regulation of TRP channels	16	2.3	0.004

Cluster 4

Category	Term	Count	FE	PValue
KEGG_PATHWAY	Nicotine addiction	15	5.2	3.27E-07

Table 3. Pathways significantly over represented in down-regulated DEG in Old vs Young PFC. The pathways were clustered by genes in common. P.Values were corrected by multiple comparisons with the DAVID methodology. Count is the number of down-regulated DEG, FE the fold enrichment, it means the additional times there are more DEG in the pathway than expected by chance.

Cluster 1

Category	Term	Count	FE	PValue
KEGG_PATHWAY	Mineral absorption	10	6.1	2.76E-05
GO_BP	cellular response to cadmium ion	6	11.5	1.19E-04
GO_BP	negative regulation of growth	6	10.3	2.13E-04
GO_BP	cellular response to zinc ion	6	10.3	2.13E-04

Cluster 2

Category	Term	Count	FE	PValue
GO_BP	positive regulation of cellular protein catabolic process	4	11.9	0.004
GO_BP	regulation of organelle assembly	3	24.5	0.005
GO_BP	positive regulation of protein localization to early endosome	3	19.6	0.008

GO_BP	establishment of endothelial barrier	4	8.2	0.011
GO_BP	positive regulation of early endosome to late endosome transport	3	12.3	0.023

Cluster 3

Category	Term	Count	FE	PValue
GO_BP	negative regulation of smoothened signaling pathway	5	8.6	0.002
GO_BP	dorsal/ventral pattern formation	6	6.1	0.003
GO_BP	smoothened signaling pathway	6	2.8	0.059

Cluster 4

Category	Term	Count	FE	PValue
GO_BP	response to interferon-beta	4	14.5	0.002
GO_BP	response to interferon-gamma	5	6.8	0.006
GO_BP	negative regulation of viral genome replication	5	4.1	0.033
GO_BP	response to interferon-alpha	3	9.8	0.035

Table 4. Pathways significantly over represented in DEG up-regulated in Old vs Young meta-analysis. The pathways were clustered by genes in common. P.Values were corrected by multiple comparisons with the DAVID methodology. Count is the number of up-regulated DEG, FE the fold enrichment, it means the additional times there are more DEG in the pathway than expected by chance.

Down-regulated pathways were located in four clusters. Cluster 1 had 34 genes which were annotated in synapse pathways. Glutamatergic synapses had a higher and more significant proportion of down-regulated genes, followed by dopaminergic and GABAergic synapses. Cholinergic and serotonergic synapses had a lower level of enrichment and higher p values. Cluster 2 had 19 genes annotated in the potassium ion transmembrane transport pathway and Cluster 3 was enriched in genes related to inter-cell communication.

Up-regulated pathways were aggregated in four clusters (Table 4). Cluster 1 had 10 genes annotated in mineral absorption, cellular response to cadmium ion and cellular response to zinc ion. Those pathways were over-represented mainly because there were seven metallothionein genes which were up-regulated and annotated in those pathways. Cluster 2 was composed of positive regulation of cellular protein catabolic process and regulation of organelle assembly, among others. It was enriched in genes of the EZR family (ezrin, radixin, and moesin). Cluster 3 contained smoothened signaling pathways, related to the sonic hedgehog (SHH) pathway. Finally, Cluster 4 was enriched in response to the interferon pathway.

4.3.5 Identification of cell types responsible for aging changes

Since PFC is a complex tissue with a combination of several types of cells, and it has been described by previous reports that different PFC cells have different responses in aging (101). We wondered which types of cells underwent greater alteration during PFC aging. We hypothesized that cells with major modifications in aging would have an over-representation of cell type specific genes in the list of DEG. Then we used the list of specific markers for neurons, oligodendrocytes and astrocytes identified by Cahoy et al. (116) (Table S5) to perform an enrichment signature analysis. The results of the analysis are shown in Table 5. On the list of down-regulated genes from the meta-analysis, there are 1.91 times more down-regulated genes from neurons than expected and 2.04 times fewer down-regulated genes from astrocytes. On the list of up-regulated genes, there are 6.67 times fewer up-regulated genes from neurons than expected and 1.77 times more up-regulated genes from astrocytes. With these results, it is possible to conclude that, in old PFC, there is a down-regulation of specific neuron genes and an up-regulation of astrocyte genes. The number of up-regulated and down-regulated DEG specific to oligodendrocytes were those expected by chance (non-significant p-value), meaning that there were no important differences in the function of those cells between old and young samples.

	Down-regulated		Up-regulated	
ID	**EF**	**Pvalue**	**EF**	**Pvalue**
Neuron	1.91	0.00E+00	-6.67	0.00E+00
Oligodendrocyte	-1.33	1.00E+00	-1.15	9.56E-01
Astrocyte	-2.04	0.00E+00	1.77	0.00E+00

Table 5. Signature analysis of specific markers of neuron, oligodendrocyte and astrocyte. EF means enrichment factor, it is the number of times that there is more genes down-regulated or up-regulated than expected by chance. Positive EF means there is an over-representation of genes of cell type, negative EF means an under-representation of genes of cell type.

4.3.6 Identification of specific neuronal regions with enrichment of down-regulated genes in aged PFC

Next, we explored which neuronal zones were more represented in the list of down-regulated genes (Table 6A). To do that we used well established markers of different zones of the neuron (Table S6). As expected according to the pathway analysis (Table 3), there were more down-regulated genes from postsynaptic (Enrichment factor, EF=3.07) and presynaptic (EF=2.13) regions than expected by chance. Interestingly, markers from other neuronal regions such as the nucleus, cytoplasm, dendritic cytoplasm or axonal cytoplasm were not over-represented. Taken together, these results suggest that, in aging, there is a specific down-regulation of synapses with less alteration in the other neuronal regions.

We discriminate the location of the DEG annotated in synapses to have a better delineation of the synapses de-regulation (Table 6B). We found that GABAergic synapse and glutamatergic synapse, the two main type of synapses in PFC had alteration in the expression of genes in presynaptic and postsynaptic regions. Interestingly, the other synapses have specific down-regulation of gene expression only in postsynaptic markers (Table S7).

A.

	Down-regulated	
ID	**EF**	**Pvalue**
Neuron Postsinaptic	3.07	2.26E-02
Neuron Presinaptic	2.13	4.30E-02
Neuron Dendritic Axonal Citoplasmatic	1.73	2.41E-01
Neuron Nuclear Citoplasmatic	-1.09	6.73E-01
Growth Cone Markers	-2.38	9.32E-01

B.

	Presynaptic	Postsynaptic	Total
GABAergic synapse	15	24	26
Glutamatergic synapse	19	20	34
Dopaminergic synapse	0	34	34
Serotoninergic synapse	0	21	22
Cholinergic synapse	7	24	24

Table 6. **(A) Signature analysis of specific neuronal regions in the down-regulated DEG.** EF means enrichment factor, it is the number of times that there is more genes down-regulated or up-regulated than expected by chance. Positive EF means there is an over-representation of genes of cell type, negative EF means an under-representation of genes of cell type. **(B) Discrimination of DEG in presynaptic and postsynaptic region.** Genes annotated in synapsis were located in pre-synaptic or postsynaptic region according KEGG database.

4.3.7 Identification of pathway enrichment in aged PFC astrocytes

Astrocyte cells had the most over-representation of specific markers in the analysis of up-regulated genes, suggesting that, in aging, there is increased activation of astrocytes. Several studies describe different ways to induce reactive astrogliosis: ischemic stroke (MCAO: middle cerebral artery occlusion) induces activation of astrocytes with a neuroprotective phenotype (A2 astrocytes), while inflammation (LPS: endotoxin LPS from *Escherichia coli* O55:B55) activates astrocytes with neurotoxic properties (A1 astrocytes) (117), (118). Additionally, methamphetamine induces premature senescence (119) and astrocyte activation (120). We mined the transcriptional signatures of the kinds of activated astrocytes previously described and compared them with our list of DEG. Table 7 summarizes the results of the over-representation analysis. The A1A2 signature comprises the up-regulated genes in activated astrocytes in general; up-regulated genes in the meta-analysis had 10 times more of those genes than expected. The down-regulated genes did not have any of those genes. This result shows that, in aging, not only is there an enrichment of astrocyte markers but those astrocytes are also active. Signatures for protective (MCAO astrocytes) and detrimental (LPS astrocytes) astrocytes were highly enriched too, with around five times more genes than expected by chance. The methamphetamine signature was not over-represented in either down-regulated or up-regulated genes.

	Down-regulated		Up-regulated	
ID	EF	Pvalue	EF	Pvalue
A1A2	NA	NA	10.13	1.99E-06
LPS astrocyte (A1)	-4.76	0.004	4.83	2.82E-05
MCAO astrocyte (A2)	-2.63	0.021	5.41	7.96E-07
Methamphetamine	1.21	0.288	-1.79	0.113

Table 7. Signature analysis of several signatures of activated astrocytes. A1A2 is the signature of astrocyte activation. EF means enrichment factor, it is the number of times that there is more genes down-regulated or up-regulated than expected by chance. Positive EF means there is an over-representation of genes of cell type, negative EF means an under-representation of genes of cell type.

Finally, the pathway analysis (Table 4) found that SHH was statistically significantly up-regulated. The SHH is a complex pathway and a recent report indicates that it is important in the interaction among neurons and astrocytes (121). We analyzed the SHH pathway in aging PFC more deeply. The SHH pathway is modulated by three transcription factors: GLI1/2/3, then we selected the transcriptional targets of GLI transcription factors using the TF2DNA database (122) (Table S8). In order to determine if the activation of the SHH pathway was limited to astrocytes, we performed the over-representation analysis with all the transcriptional targets of GLI (Gli total) and using the specific astrocyte genes (Gli astrocyte). Gli1/2/3 target genes were not over-represented in the list of DEG, but the specific astrocyte Gli1/2/3 targets were over-represented in the list of up-regulated genes with an EF of 3.18, 2.51 and 3.45, respectively (Table 8). Additionally, those lists of genes were under-represented in the list of down-regulated genes.

	Down-regulated		Up-regulated	
ID	EF	Pvalue	EF	Pvalue
Gli1 astrocyte	-1.69	0.013	3.18	2.59E-07
Gli1 total	1.12	0.034	1.02	0.471
Gli2 astrocyte	-2.17	0.001	2.51	0.001
Gli2 total	1.04	0.306	1.2	0.953
Gli3 astrocyte	-2.63	0.021	3.45	0.002
Gli3 total	1	0.528	-1.14	0.258

Table 8. Signature analysis of targets of GLI transcription factors in DEG. Gli1 total means that all the transcriptional targets of Gli1 were interrogated against the list of DEG. Similarly, Gli2 and Gli3 means the transcriptional targets of the same transcription factor. Gli1 astrocyte, Gli2 astrocyte and Gli3 astrocyte means that only the transcriptional targets present in the list of specific markers of astrocyte were used.

4.4 Discussion

4.4.1 General transcriptomic landscape of aging in PFC

The combination of old PFC vs. young PFC samples from several independent studies by meta-analysis identified a list of DEG that had high overlapping with the validation dataset constituted by a large number of biological replicates. The approach used in our study was able to detect genes with a consistent and coherent deregulation across several independent studies. The proportion of down-regulated genes vs. up-regulated genes was 2.2:1. In previous analyses of the aging transcriptomic profile on different tissues and organisms, the number and proportion of down-regulated and up-regulated genes was variable. Meta-analysis of the aged liver in mice found a 1:3 ratio of down-regulated to up-regulated genes (123). A similar result was obtained in other analysis using several aging organs -kidney, lung, brain cortex, liver- from humans, mice, and rats (102). In human lymphoblastoid cells, the proportion was 1:1 (124). Two studies using whole blood cells found a proportion close to 1.4:1 (125), (126). In a meta-analysis of human muscles, the proportion was 1.2:1 (127). This variation in the proportion of the direction of de-regulated genes could be explained as follows: since post-mitotic cells (such as muscle cells and neurons) accumulate DNA damage over their lifespan, it is more probable that mutations in transcriptionally active genes will induce a down-regulation, while mitotically active cells with an accumulation of mutations are negatively selected and removed from the tissues. Our findings support this hypothesis because the down-regulated genes had an enrichment in specific markers for neurons -post-mitotic cells- and the up-regulated genes had an enrichment in specific markers for astrocytes -cells with proliferative ability in the nervous tissue-.

In order to identify which types of PFC cells were altered in the de-regulation of the transcriptome of old samples compared with young samples, we performed on our list of DEG an over-representation and under-representation analysis with specific markers for neurons, oligodendrocytes, and astrocytes (116). As in previous studies on the cerebral cortex (101), we found an over-representation of neuronal markers in the down-regulated genes and an under-representation of those markers in the up-regulated genes. Astrocyte markers had the opposite over-representation results, with an enrichment of up-regulated genes and fewer down-regulated genes on the list of DEG. Oligodendrocyte markers had the number of DEG that would be expected by chance. Taken together, those results indicate that, in aging PFC, there is a down-regulation of neuronal genes without compensatory up-regulation of other neural genes, as well as an increased expression of astrocyte genes. Neuropathological studies show contradictory evidence regarding the change in the number of neurons and neuroglial cells in different regions of the brain with aging. Some results have pointed to a loss of neurons in the rat´s prefrontal cortex (128), basal forebrain (129), thalamus (130), cortex, hypothalamus, cerebellum and olfactory bulb (131). However, other studies found no modification in the number of neurons in aging. For instance, in the human substantia nigra, there was no correlation between the number of neurons and age (132), and in the *Rhesus* macaque, the number of white matter neurons did not show a correlation with age (133). Therefore, the down-regulation of neuron-specific markers could be explained as a result of a decreased number of neurons or a down-regulation in the expression of genes related to a specific aging phenotype. Likewise, the over-representation of astrocyte genes in the up-regulated genes is due to an increase in the number of cells or their increased activation.

Our results, as discussed below, support that in aging, there is a down-regulation of gene expression in specific neuronal zones, especially synapses, and opposite patterns of activation of astrocytes.

4.4.2 Neuron transcriptome in aged PFC: down-regulation of synapses

Specific neuron markers were over-represented in the list of down-regulated genes. The analysis of markers for specific neuron zones evidenced that in aging the more pronounced alteration involved the synapses. Genes that codified proteins from the nucleus and cytoplasm of the neuron body and neuron prolongations were not over-represented. This coincides with a previous analysis using different transcriptomic data (103) and quantitative PCR (134) where the authors reported an altered synaptic gene expression associated with chronological aging. The unbiased analysis of the down-regulated genes showed that all types of synapses were down-regulated, and it is compatible with a general dysfunction of the synaptic connectivity, modulation, and activity. When a careful analysis of the down-regulated genes was performed, a similar down-regulation of presynaptic and postsynaptic genes for GABAergic and glutamatergic synapses was found, indicating a similar involvement of excitatory and inhibitory synapses. Interestingly, for the other types of synapses -serotonergic, cholinergic and dopaminergic-, the main down-regulation was almost exclusively restricted to the postsynaptic neuron. Synaptic functions do not have the same kind of alteration. For example, genes related to the synthesis and binding of vesicles were down-regulated (SYP, SYT1, SYN2, STX1A), while genes related with docking and transport of vesicles to the membrane were up-regulated (VAMP1, SANP23) (TableS1), indicating that the presynaptic dysfunction could be restricted to specific processes.

Even though our research was based on the analysis of transcriptomic datasets, as an additional validation of our results, we found concordant results in a study using quantitative PCR in human old PFC (134). Mohan et al. reported down-regulation of interneuron and synaptic genes (calbindin, somatostatin, cholecystokinin, SLC17A7), and up-regulation of VAMP1 (134).

4.4.3 Astrocyte transcriptome in aged PFC: the opposite activation

Astrocytes, the most abundant glial cells, are important for adequate central nervous system (CNS) function. They are involved in the formation and elimination of neuronal synapses (135) (136), and also mediate the uptake and recycling of neurotransmitters (137). We found that, in aging, there is an up-regulation of specific astrocyte markers. These results coincide with a previous report using a different source of information (101). Current knowledge suggests that astrocyte number is preserved in aging (138) (139). Therefore, the up-regulation of astrocyte markers could be explained by an increase in the activation state of those cells. There are distinctive phenotypes of activated astrocytes, which depend on the stimuli that induce the activation. The best-characterized phenotypes of activated astrocytes are A1 and A2. Reactive astrocytes induced by LPS (A1 astrocytes) exhibit a phenotype that suggests they are detrimental, whereas reactive astrocytes induced by ischemia (A2 astrocytes) exhibit a cellular phenotype that suggests that they are beneficial or protective (117). The A1 and A2 phenotypes share common genes that are useful for identifying reactive astrocytes in general (activated A1A2 astrocytes). A study in rat brains found an increase of A1-like reactive astrocytes in the hippocampus and striatum with aging (99) suggesting that, in this animal model, astrocyte activation is mainly toxic and it is associated with the loss of brain function. We found that, in old

PFC, there is a strong up-regulation of A1A2 signature genes. When we analyzed what kind of activated astrocytes were present in old PFC we found a similar over-representation of A1 and A2 signature genes. Additionally, since there are reports linking methamphetamine abuse with the neurochemical profile of aging (140) and premature cellular senescence (119), therefore we compared the molecular profile of the astrocytes activated by methamphetamine abuse with our signature of old PFC, this profile was not over-represented, indicating that astrocyte activation by methamphetamine does not recapitulate normal aging astrocyte activation. These joint results indicate that aged human PFC seems to have patterns of gene-expression compatible with astrocytes activation which is heterogeneous mixing protective and toxic astrocytes.

Due to the fact that we used whole tissue with a mixture of cells in our study, we cannot delineate more precisely the proportions and specific pathways activated in each type of activated astrocyte. Single cell transcriptomic analysis of astrocytes in aging samples along with phenotypic analysis of this cells must be performed to answer this question.

However, with the pathway and signature analysis of up-regulated genes, it is possible to suggest the molecular phenotype of astrogliosis in old PFC. The fact that mineral absorption was the main up-regulated pathway in the top cluster of activated pathways was an unexpected result of the transcriptomic analysis of the CNS. However, the pathway was statistically significant, because it contained several metallothionein (MT) genes. In the meta-analysis, seven MT genes were analyzed, all of which were from the MT I family, and were up-regulated in old PFC. There is an increasing interest in the role of MT in normal and pathological CNS function. The MT superfamily has four isoforms (I to IV); isoforms I and II are expressed in the brain, mainly in astrocytes, while isoform III is expressed in neurons (141). Metallothioneins I/II are up-regulated in astrocytes in response to neuronal injury (142), and their expression is induced by several stimuli such as metals, hormones, cytokines, oxidative stress and inflammation (143). The over-expression of MTs is in general protective, for example, when MTs are overexpressed, the mouse lifespan is increased (144). Metallothioneins I/II play a neuroprotective role in several forms of brain injury and are able to augment the regenerative capacity of astrocytes (145). Metallothioneins I/II induce a form of astrogliosis that is permissive with the neurite outgrowth and associated with decreased chondroitin sulfate proteoglycan (CSPG) accumulation. CSPGs are involved in maintaining the structure and function of adult neurons, and in the regulation of proliferation, migration, and neurite outgrowth of neural stem cells in the brain. Aged rats show a significant increase in aggrecan expression throughout the PFC and in the hippocampus (146). We found up-regulation of the expression of two CSPG genes (BCAN and CD44), and thus the up-regulation of MT I could be related to an astrocyte effort to degrade the increased deposition of CSPGs as a response to synapse malfunction.

Organelle assembly, the second cluster of up-regulated genes, includes the all three ERM family proteins (ezrin, radixin, and moesin). These proteins play a crucial role in organizing membrane domains and regulating signal transduction pathways such as SHH (147). In the brain, this family is important in the regulation of plasticity and neuroprotection: ezrin (EZR) is required for the structural plasticity of peripheral astrocyte processes associated with synapses (148), moesin (MSN) regulates dendrite arborization and spine-like protrusion growth (149), and radixin (RDX) stimulates adult neural progenitor cell migration and proliferation (150). Activation of the three members of the family promotes the migration of subventricular zone-derived neuroblasts in response to traumatic brain damage (151). In old PFC, neuronal synapse dysfunction could be sensed by the astrocytes as local damage, and part of the protective

response could be the up-regulation of ERM genes. Activation of ERM proteins is mediated by RhoA in HeLa cells (152) and fibroblasts (153), but is independent of RhoA in kidney-derived cells (154). RhoA was not up-regulated in our analysis nor in previous studies (117) of old PFC, but other Rho proteins as RhoJ and RhoU were up-regulated. If those proteins can interact with ERM proteins, then it is plausible that ERM protein activation is caused by other Rho family proteins in the brain and accessory proteins such as ARHGDIA, that is also up-regulated in aging, but additional analysis of interaction of those proteins are necessary to probe this hypothesis.

Smoothened (SMO) signaling pathway, the representative pathway in the third cluster of up-regulated genes, is the intracellular effector of the activation of Sonic Hedgehog (SHH) pathway. The SHH plays a key role in the development and patterning of the CNS. In the adult brain, SHH is one of the regulators of astrocyte function and activation. Given the importance of this pathway in the biology of astrocytes, we explored in detail their complete regulation in aged PFC. SHH regulates the activity of the GLI transcription factor family, in which there are three members: GLI 1, 2 and 3, each with a different role in SHH responsive gene regulation. GLI 1 is a transcriptional activator, GLI 2 is mainly a transcriptional activator with slight repressor activity, and GLI 3 is a transcriptional repressor of target genes (155). We looked to see if the transcriptional targets of each GLI were over-represented on the list of DEG. When all the targets were interrogated, none of the lists of GLI targets were over-represented on the list of up-regulated genes and only GLI 1 targets were under-represented on the list of down-regulated genes. These results indicate that there is no general deregulation of the SHH pathway in old PFC. However, when we selected the GLI targets that are expressed specifically in astrocytes, there was an over-representation of GLI 1, 2 and 3 astrocyte targets on the list of up-regulated genes and under-representation of those targets on the list of down-regulated genes. GLI 1 and 2 are transcriptional activators and GLI3 is a repressor, then, there is an activation of GLI 1 and 2 and inactivation of GLI 3 in astrocytes in aging. Therefore, there is an activation of the SHH pathway specifically in astrocytes.

Neurons in old PFC have a wide down-regulation of expression of synaptic genes, including the genes related to biosynthesis, transport, and release of neurotransmitters. A study recently described that neurons use SHH to control different properties of the astrocytes (156) (121). SHH stimulation of Bergmann glial cells -a type of cerebellar astrocytes- promotes glutamate detection and recovery and potassium homeostasis by up-regulation of SLC1A3 (GLAST) and KCNJ10 (KIR 4.1) (156). Those genes are up-regulated in old PFC, then the activation of SHH in PFC astrocytes could be a protective response induced by down-regulation in the expression of neuronal synaptic genes. Furthermore, SHH is also involved in neural progenitor proliferation, neovascularization, and synaptogenesis (157). SHH reduces astrocyte reactivity and the inflammatory response after a brain injury (157), and astrocytes stimulated by SHH protect neurons from cell death (121). This is compatible with the finding of over-representation of the protective astrocyte signature on the list of up-regulated genes.

On the other hand, we found an over-representation of the neurotoxic astrocyte signature, suggesting that there are parallel pathways of astrocyte activation inducing diverse astrocyte phenotypes in brain aging. Our analysis identified up-regulation of related inflammatory pathways (the Cluster 4 of up-regulated genes). This cluster consisted of the enrichment in genes annotated in response to interferon alpha, beta, and gamma. In the aging brain, it is well characterized that interferon signaling at the choroid plexus negatively affects brain function

(158) and that the interferon pathways are induced in LPS-reactive astrogliosis (117). Inflammation is one of the hallmarks of aging, and the hypothalamus integrates inflammatory responses with systemic control of aging through nuclear factor kB (NF-kB) and microglia-neuron neuroimmune crosstalk (159) (160). Inflammation is so important in aging brains, that chronic treatment with an IFN-I activator contributes to the development of neurodegenerative disease in wild-type mice (161). In the context of astrocytes, neurotoxic phenotype development after exposure to LPS is characterized by the induction of interferon pathways (117). The activation of IFN pathways is also compatible with the aging model which describes inflammatory astrocyte (A1) activation. Moreover, the direct analysis of astrocytes in normal aging showed that one of the up-regulated pathways in mouse old brain astrocytes was interferon signaling (99).

These results suggest that the up-regulated pathways we found were mainly due to astrocyte activation and they represent two divergent astrocytes molecular y cellular phenotypes.

4.4.4 Conclusion

Meta-analysis of transcriptomic data increases the statistical power of the individual datasets and, in addition, is able to identify DEG which are consistently de-regulated across the different experiments. A big advantage of this approach is that the particular characteristics of each dataset are unmasked and only the common processes for all datasets are revealed. In our analysis, we detected that neurons are some of the most important cells affected by aging in the PFC, and, in accordance with other researchers, we delineated the biggest impairment in synapse function, with specific variations depending on the type of synapses. Additionally, using the over-representation and under-representation analysis of curated expression signatures we identified that there are heterogeneous transcriptomic profiles associated with the activation of astrocytes. We found evidence of at least two different phenotypes of activated astrogliosis: A1 (neurotoxic) and A2 (neuroprotective). Due to our analysis design, we cannot identify the chronological order or magnitude of those alterations, but the results are consistent with the normal cognitive decline associated with aging. A plausible hypothesis is that neurons, post-mitotic cells accumulated DNA damage for decades, and then they expressed a phenotype characterized by synapsis dysfunction. As a response of that, there are activation of astrocytes in at least two different pathways: A1 and A2 astrocytes.

We propose a model (Figure 4) where synapses in normal aged PFC are in two states: some synapses are deleteriously related to A1 astrocytes and others are protectively related to A2 astrocytes. A1 astrocytes are the result of activation by aging-related inflammation and A2 astrocytes could be activated as a response to the switch-off of the synapses.

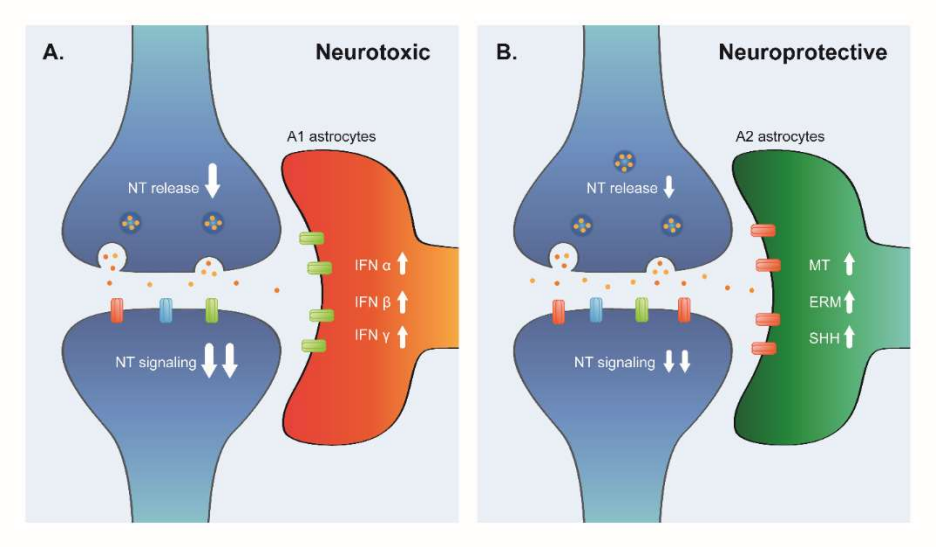

Figure 4. Model of tripartite synapse in old PFC. In old PFC there is a down-regulation of expression of presynaptic genes in GABAergic and Glutamatergic synapses and down-regulation of post-synaptic genes in all kind of synapses. They are in two divergent environments (A) The presence of A1 astrocytes induces a neurotoxic phenotype, those astrocytes have an activation of inflammatory response represented by interferon pathways. (B) There are also A2 astrocytes in old PFC. A2 astrocytes have activation of metallothioneins, EZR and SHH pathways. Those pathways are pro-synaptogenic and neuroprotective, then, the alteration in the function of the synapses will be less severe than in (A).

There are several questions remaining: what is the origin of synapse down-regulation? Is the astrocytes phenotypes fixed or can they change with time or stimuli? What is the extent of A1 and A2 activation? How is the local synapse environment under A1 or A2 astrocyte regulatory control? And finally, what is the situation of this complex relationship between neurons and reactive astrocytes in neurodegenerative diseases?

5. GENERAL CONCLUSIONS

Aging, a ubiquitous biological process, is the greatest risk factor for morbidity and mortality in developed countries. It is associated with increased rates of cardiovascular disease, cancer and neurodegenerative disease among others. One of the biggest dreams of humanity for a long time has been to delay, stop or for the most optimistic, reverse the deterioration of function and physiology associated with time.

The current state of knowledge understands aging as a complex phenotype that depends on the interaction of several factors. The study of complex processes requires the use of integrative tools as the omics and the systems biology.

The main presumption at the beginning of this research was that accumulation of DNA damage is an important player in the aging and the modulation of the ability to repair the damage is able to modify the evolution of the phenotype.

With the experience acquired analyzing several datasets of transcriptomic from old mice and humans with normal and abnormal phenotype the first conclusion that emerges is that even at a first glance aging looks like noisy and stochastic phenomena there is an internal consistency and common processes. To make evident the molecular mechanisms of aging is necessary to use the appropriate techniques with a bit of creativity.

The study of the phenotypic and transcriptomic response to the dietary interventions that induces renal IRI identified that aged mice are able to activate a similar but reduce protection against acute stress. It is a positive result because indicate that old organisms can be beneficiated of interventions that modulate pathways related to healthy aging. Indeed, a pilot study was showed that old donor receptors of renal transplant had beneficial outcomes of a short time calorie and protein restriction diet (162).

The identification that different dietary interventions are able to induce the same stress protection by common pathways reinforces the idea that aging and related phenotypes depend on evolutionarily conserved pathways. The parallel study of the transcriptional protective responses pointed to a set of promising pathways (retinoid X receptor, the farnesoid X receptor, and the pregnane X receptor) involved in increased resistance to stress and probably in the survival response related to the extension of lifespan.

The direct connection between a limited capability to repair the DNA damage (Ercc1Δ/+ mice) and neurodegenerative diseases as Parkinson gives, in the opposite sense that previous results, more experimental evidence that connect the accumulation of DNA damage in transcriptionally active genes with aging. The combination of next-generation transcriptomic with exhaustive phenotypic characterization confirmed the identification of a powerful animal model of sporadic Parkinson. The larger enrichment of down-regulated pathways in common with transcriptomic of patients with the disease generates an opportunity to explore environmental factors interacting with the genetic factors in the developing of neurodegenerative diseases that could be related with the up-regulation of specific pathways.

Finally, the integrative analysis of several independent studies of the transcriptome of the prefrontal cortex of normal aging people evidences that in normal aging also there are common and conserved mechanisms. It is an example of how the omics technologies can identify relevant pathways to improve the knowledge of complex phenotypes. The identification of protective and neurotoxic astrocytes in the old brain and the description of the molecular signatures and de-pathways is the first step to develop pharmacological interventions to modulate the aging.

6. RECOMMENDATIONS AND PROSPECTS

The main findings of this research conformed the initial steps to get more in deep in the comprehension molecular mechanisms of aging. The final objective of any research in aging in to develop strategies able to modify the natural progression of the associated phenotypes to the age and to avoid the apparition of chronic diseases.
In my opinion, three promising results need additional research to move in the study to understand how they can be modulated. First, pharmacological activation of the family of X receptors and how then are able to activated the survival response. What are the effects at short and long time? Second, additional exploration of the transcriptomic response of the substantia nigra of Ercc1Δ/+ mice at different ages and expose at molecules able to interact with the genotype to produces Parkinson´s disease. And finally, a better description of the protective and non-protective astrocytes and the exploration of molecules able to activate the pathways identified in A2 astrocytes.

7. REFERENCES

1. Mendonca GV, Pezarat-Correia P, Vaz JR, Silva L, Heffernan KS. Impact of Aging on Endurance and Neuromuscular Physical Performance: The Role of Vascular Senescence. Sports Med. 2017;47(4):583-98.
2. Vermeij WP, Hoeijmakers JH, Pothof J. Aging: not all DNA damage is equal. Curr Opin Genet Dev. 2014;26:124-30.
3. Hoeijmakers JH. DNA damage, aging, and cancer. N Engl J Med. 2009;361(15):1475-85.
4. Brown-Borg HM. Longevity in mice: is stress resistance a common factor? Age (Dordr). 2006;28(2):145-62.
5. Mitchell JR, Verweij M, Brand K, van de Ven M, Goemaere N, van den Engel S, et al. Short-term dietary restriction and fasting precondition against ischemia reperfusion injury in mice. Aging Cell. 2010;9(1):40-53.
6. Susa D, Mitchell JR, Verweij M, van de Ven M, Roest H, van den Engel S, et al. Congenital DNA repair deficiency results in protection against renal ischemia reperfusion injury in mice. Aging Cell. 2009;8(2):192-200.
7. Schumacher B, van der Pluijm I, Moorhouse MJ, Kosteas T, Robinson AR, Suh Y, et al. Delayed and accelerated aging share common longevity assurance mechanisms. PLoS Genet. 2008;4(8):e1000161.
8. Cole JH, Franke K. Predicting Age Using Neuroimaging: Innovative Brain Ageing Biomarkers. Trends Neurosci. 2017;40(12):681-90.
9. López-Otín C, Blasco MA, Partridge L, Serrano M, Kroemer G. The hallmarks of aging. Cell. 2013;153(6):1194-217.
10. Bjorksten J, Tenhu H. The crosslinking theory of aging--added evidence. Exp Gerontol. 1990;25(2):91-5.
11. Afanas'ev I. Signaling and Damaging Functions of Free Radicals in Aging-Free Radical Theory, Hormesis, and TOR. Aging Dis. 2010;1(2):75-88.
12. Wei W, Ji S. Cellular senescence: Molecular mechanisms and pathogenicity. J Cell Physiol. 2018;233(12):9121-35.
13. Roche Y, Zhang D, Segers-Nolten GM, Vermeulen W, Wyman C, Sugasawa K, et al. Fluorescence correlation spectroscopy of the binding of nucleotide excision repair protein XPC-hHr23B with DNA substrates. J Fluoresc. 2008;18(5):987-95.
14. Mitchell JR, Hoeijmakers JH, Niedernhofer LJ. Divide and conquer: nucleotide excision repair battles cancer and ageing. Curr Opin Cell Biol. 2003;15(2):232-40.
15. Diderich KE, Nicolaije C, Priemel M, Waarsing JH, Day JS, Brandt RM, et al. Bone fragility and decline in stem cells in prematurely aging DNA repair deficient trichothiodystrophy mice. Age (Dordr). 2012;34(4):845-61.
16. Nagtegaal AP, Rainey RN, van der Pluijm I, Brandt RM, van der Horst GT, Borst JG, et al. Cockayne syndrome group B (Csb) and group a (Csa) deficiencies predispose to hearing loss and cochlear hair cell degeneration in mice. J Neurosci. 2015;35(10):4280-6.
17. Jaarsma D, van der Pluijm I, van der Horst GT, Hoeijmakers JH. Cockayne syndrome pathogenesis: lessons from mouse models. Mech Ageing Dev. 2013;134(5-6):180-95.
18. van der Pluijm I, Garinis GA, Brandt RM, Gorgels TG, Wijnhoven SW, Diderich KE, et al. Impaired genome maintenance suppresses the growth hormone--insulin-like growth factor 1 axis in mice with Cockayne syndrome. PLoS Biol. 2007;5(1):e2.

19. Niedernhofer LJ, Garinis GA, Raams A, Lalai AS, Robinson AR, Appeldoorn E, et al. A new progeroid syndrome reveals that genotoxic stress suppresses the somatotroph axis. Nature. 2006;444(7122):1038-43.
20. Spoor M, Nagtegaal AP, Ridwan Y, Borgesius NZ, van Alphen B, van der Pluijm I, et al. Accelerated loss of hearing and vision in the DNA-repair deficient Ercc1(δ/-) mouse. Mech Ageing Dev. 2012;133(2-3):59-67.
21. Vo N, Seo HY, Robinson A, Sowa G, Bentley D, Taylor L, et al. Accelerated aging of intervertebral discs in a mouse model of progeria. J Orthop Res. 2010;28(12):1600-7.
22. Schermer B, Bartels V, Frommolt P, Habermann B, Braun F, Schultze JL, et al. Transcriptional profiling reveals progeroid Ercc1(-/Δ) mice as a model system for glomerular aging. BMC Genomics. 2013;14:559.
23. Garinis GA, Uittenboogaard LM, Stachelscheid H, Fousteri M, van Ijcken W, Breit TM, et al. Persistent transcription-blocking DNA lesions trigger somatic growth attenuation associated with longevity. Nat Cell Biol. 2009;11(5):604-15.
24. Madabhushi R, Pan L, Tsai LH. DNA damage and its links to neurodegeneration. Neuron. 2014;83(2):266-82.
25. Martin LJ. DNA damage and repair: relevance to mechanisms of neurodegeneration. J Neuropathol Exp Neurol. 2008;67(5):377-87.
26. Sepe S, Payan-Gomez C, Milanese C, Hoeijmakers JH, Mastroberardino PG. Nucleotide excision repair in chronic neurodegenerative diseases. DNA Repair (Amst). 2013;12(8):568-77.
27. Borgesius NZ, de Waard MC, van der Pluijm I, Omrani A, Zondag GC, van der Horst GT, et al. Accelerated age-related cognitive decline and neurodegeneration, caused by deficient DNA repair. J Neurosci. 2011;31(35):12543-53.
28. Hirsch E, Graybiel AM, Agid YA. Melanized dopaminergic neurons are differentially susceptible to degeneration in Parkinson's disease. Nature. 1988;334(6180):345-8.
29. Ferrante RJ, Kowall NW, Beal MF, Richardson EP, Bird ED, Martin JB. Selective sparing of a class of striatal neurons in Huntington's disease. Science. 1985;230(4725):561-3.
30. Braak H, Alafuzoff I, Arzberger T, Kretzschmar H, Del Tredici K. Staging of Alzheimer disease-associated neurofibrillary pathology using paraffin sections and immunocytochemistry. Acta Neuropathol. 2006;112(4):389-404.
31. Fontana L, Partridge L, Longo VD. Extending healthy life span--from yeast to humans. Science. 2010;328(5976):321-6.
32. Fontana L, Nehme J, Demaria M. Caloric restriction and cellular senescence. Mech Ageing Dev. 2018;176:19-23.
33. López-Lluch G, Navas P. Calorie restriction as an intervention in ageing. J Physiol. 2016;594(8):2043-60.
34. Omodei D, Licastro D, Salvatore F, Crosby SD, Fontana L. Serum from humans on long-term calorie restriction enhances stress resistance in cell culture. Aging (Albany NY). 2013;5(8):599-606.
35. Huisman SA, de Bruijn P, Ghobadi Moghaddam-Helmantel IM, IJzermans JN, Wiemer EA, Mathijssen RH, et al. Fasting protects against the side effects of irinotecan treatment but does not affect anti-tumour activity in mice. Br J Pharmacol. 2016;173(5):804-14.
36. Antoine DJ, Williams DP, Kipar A, Laverty H, Park BK. Diet restriction inhibits apoptosis and HMGB1 oxidation and promotes inflammatory cell recruitment during acetaminophen hepatotoxicity. Mol Med. 2010;16(11-12):479-90.
37. Verweij M, van de Ven M, Mitchell JR, van den Engel S, Hoeijmakers JH, Ijzermans JN, et al. Glucose supplementation does not interfere with fasting-induced protection against renal ischemia/reperfusion injury in mice. Transplantation. 2011;92(7):752-8.

38. Isenberg JS, Roberts DD. The role of CD47 in pathogenesis and treatment of renal ischemia reperfusion injury. Pediatr Nephrol. 2018.
39. Situmorang GR, Sheerin NS. Ischaemia reperfusion injury: mechanisms of progression to chronic graft dysfunction. Pediatr Nephrol. 2018.
40. Kezić A, Stajic N, Thaiss F. Innate Immune Response in Kidney Ischemia/Reperfusion Injury: Potential Target for Therapy. J Immunol Res. 2017;2017:6305439.
41. Barin-Le Guellec C, Largeau B, Bon D, Marquet P, Hauet T. Ischemia/reperfusion-associated tubular cells injury in renal transplantation: Can metabolomics inform about mechanisms and help identify new therapeutic targets? Pharmacol Res. 2018;129:34-43.
42. Bonventre JV, Yang L. Cellular pathophysiology of ischemic acute kidney injury. J Clin Invest. 2011;121(11):4210-21.
43. Jongbloed F, de Bruin RW, Pennings JL, Payán-Gómez C, van den Engel S, van Oostrom CT, et al. Preoperative fasting protects against renal ischemia-reperfusion injury in aged and overweight mice. PLoS One. 2014;9(6):e100853.
44. Jongbloed F, Saat TC, Verweij M, Payan-Gomez C, Hoeijmakers JH, van den Engel S, et al. A signature of renal stress resistance induced by short-term dietary restriction, fasting, and protein restriction. Sci Rep. 2017;7:40901.
45. Kilkenny C, Browne WJ, Cuthill IC, Emerson M, Altman DG. Improving bioscience research reporting: the ARRIVE guidelines for reporting animal research. PLoS Biol. 2010;8(6):e1000412.
46. Ringnér M. What is principal component analysis? Nat Biotechnol. 2008;26(3):303-4.
47. Huber W, Carey VJ, Gentleman R, Anders S, Carlson M, Carvalho BS, et al. Orchestrating high-throughput genomic analysis with Bioconductor. Nat Methods. 2015;12(2):115-21.
48. Xia J, Fjell CD, Mayer ML, Pena OM, Wishart DS, Hancock RE. INMEX--a web-based tool for integrative meta-analysis of expression data. Nucleic Acids Res. 2013;41(Web Server issue):W63-70.
49. Sinclair DA. Toward a unified theory of caloric restriction and longevity regulation. Mech Ageing Dev. 2005;126(9):987-1002.
50. Estrela GR, Wasinski F, Batista RO, Hiyane MI, Felizardo RJ, Cunha F, et al. Caloric Restriction Is More Efficient than Physical Exercise to Protect from Cisplatin Nephrotoxicity via PPAR-Alpha Activation. Front Physiol. 2017;8:116.
51. Martinez-Jimenez CP, Eling N, Chen HC, Vallejos CA, Kolodziejczyk AA, Connor F, et al. Aging increases cell-to-cell transcriptional variability upon immune stimulation. Science. 2017;355(6332):1433-6.
52. Enge M, Arda HE, Mignardi M, Beausang J, Bottino R, Kim SK, et al. Single-Cell Analysis of Human Pancreas Reveals Transcriptional Signatures of Aging and Somatic Mutation Patterns. Cell. 2017;171(2):321-30.e14.
53. Ein-Dor L, Zuk O, Domany E. Thousands of samples are needed to generate a robust gene list for predicting outcome in cancer. Proc Natl Acad Sci U S A. 2006;103(15):5923-8.
54. Hong G, Zhang W, Li H, Shen X, Guo Z. Separate enrichment analysis of pathways for up- and downregulated genes. J R Soc Interface. 2014;11(92):20130950.
55. Goldstein JL, Zhao TJ, Li RL, Sherbet DP, Liang G, Brown MS. Surviving starvation: essential role of the ghrelin-growth hormone axis. Cold Spring Harb Symp Quant Biol. 2011;76:121-7.
56. Wu G, Fang YZ, Yang S, Lupton JR, Turner ND. Glutathione metabolism and its implications for health. J Nutr. 2004;134(3):489-92.
57. Chen Y, Dong H, Thompson DC, Shertzer HG, Nebert DW, Vasiliou V. Glutathione defense mechanism in liver injury: insights from animal models. Food Chem Toxicol. 2013;60:38-44.
58. Lou Z, Wang AP, Duan XM, Hu GH, Song GL, Zuo ML, et al. Upregulation of NOX2 and NOX4 Mediated by TGF-β Signaling Pathway Exacerbates Cerebral Ischemia/Reperfusion Oxidative Stress Injury. Cell Physiol Biochem. 2018;46(5):2103-13.

59. Martinez BA, Petersen DA, Gaeta AL, Stanley SP, Caldwell GA, Caldwell KA. Dysregulation of the Mitochondrial Unfolded Protein Response Induces Non-Apoptotic Dopaminergic Neurodegeneration in. J Neurosci. 2017;37(46):11085-100.
60. Olivera-Perez HM, Lam L, Dang J, Jiang W, Rodriguez F, Rigali E, et al. Omega-3 fatty acids increase the unfolded protein response and improve amyloid-β phagocytosis by macrophages of patients with mild cognitive impairment. FASEB J. 2017;31(10):4359-69.
61. Peng W, Robertson L, Gallinetti J, Mejia P, Vose S, Charlip A, et al. Surgical stress resistance induced by single amino acid deprivation requires Gcn2 in mice. Sci Transl Med. 2012;4(118):118ra11.
62. Longo VD, Antebi A, Bartke A, Barzilai N, Brown-Borg HM, Caruso C, et al. Interventions to Slow Aging in Humans: Are We Ready? Aging Cell. 2015;14(4):497-510.
63. Masoro EJ. Caloric restriction and aging: controversial issues. J Gerontol A Biol Sci Med Sci. 2006;61(1):14-9.
64. Dang W. The controversial world of sirtuins. Drug Discov Today Technol. 2014;12:e9-e17.
65. Meijer AJ, Lorin S, Blommaart EF, Codogno P. Regulation of autophagy by amino acids and MTOR-dependent signal transduction. Amino Acids. 2015;47(10):2037-63.
66. Valente E, Rocha M. Integrating data from heterogeneous DNA microarray platforms. J Integr Bioinform. 2015;12(4):281.
67. McCall MN, Jaffee HA, Irizarry RA. fRMA ST: frozen robust multiarray analysis for Affymetrix Exon and Gene ST arrays. Bioinformatics. 2012;28(23):3153-4.
68. Carty CL, Kooperberg C, Neuhouser ML, Tinker L, Howard B, Wactawski-Wende J, et al. Low-fat dietary pattern and change in body-composition traits in the Women's Health Initiative Dietary Modification Trial. Am J Clin Nutr. 2011;93(3):516-24.
69. Beresford SA, Johnson KC, Ritenbaugh C, Lasser NL, Snetselaar LG, Black HR, et al. Low-fat dietary pattern and risk of colorectal cancer: the Women's Health Initiative Randomized Controlled Dietary Modification Trial. JAMA. 2006;295(6):643-54.
70. Prentice RL, Caan B, Chlebowski RT, Patterson R, Kuller LH, Ockene JK, et al. Low-fat dietary pattern and risk of invasive breast cancer: the Women's Health Initiative Randomized Controlled Dietary Modification Trial. JAMA. 2006;295(6):629-42.
71. Huang dW, Sherman BT, Lempicki RA. Bioinformatics enrichment tools: paths toward the comprehensive functional analysis of large gene lists. Nucleic Acids Res. 2009;37(1):1-13.
72. Tseng GC, Ghosh D, Feingold E. Comprehensive literature review and statistical considerations for microarray meta-analysis. Nucleic Acids Res. 2012;40(9):3785-99.
73. Seo J, Gordish-Dressman H, Hoffman EP. An interactive power analysis tool for microarray hypothesis testing and generation. Bioinformatics. 2006;22(7):808-14.
74. Lee SE, Koo YD, Lee JS, Kwak SH, Jung HS, Cho YM, et al. Retinoid X receptor α overexpression alleviates mitochondrial dysfunction-induced insulin resistance through transcriptional regulation of insulin receptor substrate 1. Mol Cells. 2015;38(4):356-61.
75. Amigo I, Kowaltowski AJ. Dietary restriction in cerebral bioenergetics and redox state. Redox Biol. 2014;2:296-304.
76. Choi BK, Kim JH, Jung JS, Lee YS, Han ME, Baek SY, et al. Reduction of ischemia-induced cerebral injury by all-trans-retinoic acid. Exp Brain Res. 2009;193(4):581-9.
77. Shen H, Luo Y, Kuo CC, Deng X, Chang CF, Harvey BK, et al. 9-Cis-retinoic acid reduces ischemic brain injury in rodents via bone morphogenetic protein. J Neurosci Res. 2009;87(2):545-55.
78. Fusco S, Pani G. Brain response to calorie restriction. Cell Mol Life Sci. 2013;70(17):3157-70.
79. Ali AH, Carey EJ, Lindor KD. Recent advances in the development of farnesoid X receptor agonists. Ann Transl Med. 2015;3(1):5.
80. Mellon I. Transcription-coupled repair: a complex affair. Mutat Res. 2005;577(1-2):155-61.

81. Jaarsma D, van der Pluijm I, de Waard MC, Haasdijk ED, Brandt R, Vermeij M, et al. Age-related neuronal degeneration: complementary roles of nucleotide excision repair and transcription-coupled repair in preventing neuropathology. PLoS Genet. 2011;7(12):e1002405.
82. Kraemer KH, Patronas NJ, Schiffmann R, Brooks BP, Tamura D, DiGiovanna JJ. Xeroderma pigmentosum, trichothiodystrophy and Cockayne syndrome: a complex genotype-phenotype relationship. Neuroscience. 2007;145(4):1388-96.
83. DelleDonne A, Klos KJ, Fujishiro H, Ahmed Z, Parisi JE, Josephs KA, et al. Incidental Lewy body disease and preclinical Parkinson disease. Arch Neurol. 2008;65(8):1074-80.
84. Sepe S, Milanese C, Gabriels S, Derks KW, Payan-Gomez C, van IJcken WF, et al. Inefficient DNA Repair Is an Aging-Related Modifier of Parkinson's Disease. Cell Rep. 2016;15(9):1866-75.
85. Ahmad A, Robinson AR, Duensing A, van Drunen E, Beverloo HB, Weisberg DB, et al. ERCC1-XPF endonuclease facilitates DNA double-strand break repair. Mol Cell Biol. 2008;28(16):5082-92.
86. Brouwer RW, van den Hout MC, Grosveld FG, van Ijcken WF. NARWHAL, a primary analysis pipeline for NGS data. Bioinformatics. 2012;28(2):284-5.
87. Xu G, Deng N, Zhao Z, Judeh T, Flemington E, Zhu D. SAMMate: a GUI tool for processing short read alignments in SAM/BAM format. Source Code Biol Med. 2011;6(1):2.
88. Zheng B, Liao Z, Locascio JJ, Lesniak KA, Roderick SS, Watt ML, et al. PGC-1α, a potential therapeutic target for early intervention in Parkinson's disease. Sci Transl Med. 2010;2(52):52ra73.
89. Xiao Y, Hsiao TH, Suresh U, Chen HI, Wu X, Wolf SE, et al. A novel significance score for gene selection and ranking. Bioinformatics. 2014;30(6):801-7.
90. Subramanian A, Kuehn H, Gould J, Tamayo P, Mesirov JP. GSEA-P: a desktop application for Gene Set Enrichment Analysis. Bioinformatics. 2007;23(23):3251-3.
91. Vivar JC, Pemu P, McPherson R, Ghosh S. Redundancy control in pathway databases (ReCiPa): an application for improving gene-set enrichment analysis in Omics studies and "Big data" biology. OMICS. 2013;17(8):414-22.
92. Mutez E, Nkiliza A, Belarbi K, de Broucker A, Vanbesien-Mailliot C, Bleuse S, et al. Involvement of the immune system, endocytosis and EIF2 signaling in both genetically determined and sporadic forms of Parkinson's disease. Neurobiol Dis. 2014;63:165-70.
93. Mootha VK, Lindgren CM, Eriksson KF, Subramanian A, Sihag S, Lehar J, et al. PGC-1alpha-responsive genes involved in oxidative phosphorylation are coordinately downregulated in human diabetes. Nat Genet. 2003;34(3):267-73.
94. Eden E, Navon R, Steinfeld I, Lipson D, Yakhini Z. GOrilla: a tool for discovery and visualization of enriched GO terms in ranked gene lists. BMC Bioinformatics. 2009;10:48.
95. Milanese C, Cerri S, Ulusoy A, Gornati SV, Plat A, Gabriels S, et al. Activation of the DNA damage response in vivo in synucleinopathy models of Parkinson's disease. Cell Death Dis. 2018;9(8):818.
96. Vermeij WP, Dollé ME, Reiling E, Jaarsma D, Payan-Gomez C, Bombardieri CR, et al. Restricted diet delays accelerated ageing and genomic stress in DNA-repair-deficient mice. Nature. 2016;537(7620):427-31.
97. Caspers S, Moebus S, Lux S, Pundt N, Schütz H, Mühleisen TW, et al. Studying variability in human brain aging in a population-based German cohort-rationale and design of 1000BRAINS. Front Aging Neurosci. 2014;6:149.
98. Lemaitre H, Goldman AL, Sambataro F, Verchinski BA, Meyer-Lindenberg A, Weinberger DR, et al. Normal age-related brain morphometric changes: nonuniformity across cortical thickness, surface area and gray matter volume? Neurobiol Aging. 2012;33(3):617.e1-9.
99. Clarke LE, Liddelow SA, Chakraborty C, Münch AE, Heiman M, Barres BA. Normal aging induces A1-like astrocyte reactivity. Proc Natl Acad Sci U S A. 2018;115(8):E1896-E905.

100. Chen CY, Logan RW, Ma T, Lewis DA, Tseng GC, Sibille E, et al. Effects of aging on circadian patterns of gene expression in the human prefrontal cortex. Proc Natl Acad Sci U S A. 2016;113(1):206-11.
101. Rhinn H, Abeliovich A. Differential Aging Analysis in Human Cerebral Cortex Identifies Variants in TMEM106B and GRN that Regulate Aging Phenotypes. Cell Syst. 2017;4(4):404-15.e5.
102. de Magalhães JP, Curado J, Church GM. Meta-analysis of age-related gene expression profiles identifies common signatures of aging. Bioinformatics. 2009;25(7):875-81.
103. Dillman AA, Majounie E, Ding J, Gibbs JR, Hernandez D, Arepalli S, et al. Transcriptomic profiling of the human brain reveals that altered synaptic gene expression is associated with chronological aging. Sci Rep. 2017;7(1):16890.
104. Eijssen LM, Jaillard M, Adriaens ME, Gaj S, de Groot PJ, Müller M, et al. User-friendly solutions for microarray quality control and pre-processing on ArrayAnalysis.org. Nucleic Acids Res. 2013;41(Web Server issue):W71-6.
105. Ritchie ME, Phipson B, Wu D, Hu Y, Law CW, Shi W, et al. limma powers differential expression analyses for RNA-sequencing and microarray studies. Nucleic Acids Res. 2015;43(7):e47.
106. Johnson WE, Li C, Rabinovic A. Adjusting batch effects in microarray expression data using empirical Bayes methods. Biostatistics. 2007;8(1):118-27.
107. Wang X, Kang DD, Shen K, Song C, Lu S, Chang LC, et al. An R package suite for microarray meta-analysis in quality control, differentially expressed gene analysis and pathway enrichment detection. Bioinformatics. 2012;28(19):2534-6.
108. Rhodes DR, Barrette TR, Rubin MA, Ghosh D, Chinnaiyan AM. Meta-analysis of microarrays: interstudy validation of gene expression profiles reveals pathway dysregulation in prostate cancer. Cancer Res. 2002;62(15):4427-33.
109. Wang J, Duncan D, Shi Z, Zhang B. WEB-based GEne SeT AnaLysis Toolkit (WebGestalt): update 2013. Nucleic Acids Res. 2013;41(Web Server issue):W77-83.
110. Lanz TA, Joshi JJ, Reinhart V, Johnson K, Grantham LE, Volfson D. STEP levels are unchanged in pre-frontal cortex and associative striatum in post-mortem human brain samples from subjects with schizophrenia, bipolar disorder and major depressive disorder. PLoS One. 2015;10(3):e0121744.
111. Somel M, Franz H, Yan Z, Lorenc A, Guo S, Giger T, et al. Transcriptional neoteny in the human brain. Proc Natl Acad Sci U S A. 2009;106(14):5743-8.
112. Maycox PR, Kelly F, Taylor A, Bates S, Reid J, Logendra R, et al. Analysis of gene expression in two large schizophrenia cohorts identifies multiple changes associated with nerve terminal function. Mol Psychiatry. 2009;14(12):1083-94.
113. Somel M, Guo S, Fu N, Yan Z, Hu HY, Xu Y, et al. MicroRNA, mRNA, and protein expression link development and aging in human and macaque brain. Genome Res. 2010;20(9):1207-18.
114. Walsh CJ, Hu P, Batt J, Santos CC. Microarray Meta-Analysis and Cross-Platform Normalization: Integrative Genomics for Robust Biomarker Discovery. Microarrays (Basel). 2015;4(3):389-406.
115. Heberle H, Meirelles GV, da Silva FR, Telles GP, Minghim R. InteractiVenn: a web-based tool for the analysis of sets through Venn diagrams. BMC Bioinformatics. 2015;16:169.
116. Cahoy JD, Emery B, Kaushal A, Foo LC, Zamanian JL, Christopherson KS, et al. A transcriptome database for astrocytes, neurons, and oligodendrocytes: a new resource for understanding brain development and function. J Neurosci. 2008;28(1):264-78.
117. Zamanian JL, Xu L, Foo LC, Nouri N, Zhou L, Giffard RG, et al. Genomic analysis of reactive astrogliosis. J Neurosci. 2012;32(18):6391-410.
118. Liddelow SA, Guttenplan KA, Clarke LE, Bennett FC, Bohlen CJ, Schirmer L, et al. Neurotoxic reactive astrocytes are induced by activated microglia. Nature. 2017;541(7638):481-7.

119. Astarita G, Avanesian A, Grimaldi B, Realini N, Justinova Z, Panlilio LV, et al. Methamphetamine accelerates cellular senescence through stimulation of de novo ceramide biosynthesis. PLoS One. 2015;10(2):e0116961.
120. Bortell N, Basova L, Semenova S, Fox HS, Ravasi T, Marcondes MC. Astrocyte-specific overexpressed gene signatures in response to methamphetamine exposure in vitro. J Neuroinflammation. 2017;14(1):49.
121. Ugbode CI, Smith I, Whalley BJ, Hirst WD, Rattray M. Sonic hedgehog signalling mediates astrocyte crosstalk with neurons to confer neuroprotection. J Neurochem. 2017;142(3):429-43.
122. Pujato M, Kieken F, Skiles AA, Tapinos N, Fiser A. Prediction of DNA binding motifs from 3D models of transcription factors; identifying TLX3 regulated genes. Nucleic Acids Res. 2014;42(22):13500-12.
123. Lee JS, Ward WO, Ren H, Vallanat B, Darlington GJ, Han ES, et al. Meta-analysis of gene expression in the mouse liver reveals biomarkers associated with inflammation increased early during aging. Mech Ageing Dev. 2012;133(7):467-78.
124. Harris SE, Riggio V, Evenden L, Gilchrist T, McCafferty S, Murphy L, et al. Age-related gene expression changes, and transcriptome wide association study of physical and cognitive aging traits, in the Lothian Birth Cohort 1936. Aging (Albany NY). 2017;9(12):2489-503.
125. Bryois J, Buil A, Ferreira PG, Panousis NI, Brown AA, Viñuela A, et al. Time-dependent genetic effects on gene expression implicate aging processes. Genome Res. 2017;27(4):545-52.
126. Reynolds LM, Ding J, Taylor JR, Lohman K, Soranzo N, de la Fuente A, et al. Transcriptomic profiles of aging in purified human immune cells. BMC Genomics. 2015;16:333.
127. Voutetakis K, Chatziioannou A, Gonos ES, Trougakos IP. Comparative Meta-Analysis of Transcriptomics Data during Cellular Senescence and In Vivo Tissue Ageing. Oxid Med Cell Longev. 2015;2015:732914.
128. Stranahan AM, Jiam NT, Spiegel AM, Gallagher M. Aging reduces total neuron number in the dorsal component of the rodent prefrontal cortex. J Comp Neurol. 2012;520(6):1318-26.
129. Wellman CL, Sengelaub DR. Alterations in dendritic morphology of frontal cortical neurons after basal forebrain lesions in adult and aged rats. Brain Res. 1995;669(1):48-58.
130. Diaz F, Villena A, Gonzalez P, Requena V, Rius F, Perez De Vargas I. Stereological age-related changes in neurons of the rat dorsal lateral geniculate nucleus. Anat Rec. 1999;255(4):396-400.
131. Morterá P, Herculano-Houzel S. Age-related neuronal loss in the rat brain starts at the end of adolescence. Front Neuroanat. 2012;6:45.
132. Di Lorenzo Alho AT, Suemoto CK, Polichiso L, Tampellini E, de Oliveira KC, Molina M, et al. Three-dimensional and stereological characterization of the human substantia nigra during aging. Brain Struct Funct. 2016;221(7):3393-403.
133. Mortazavi F, Wang X, Rosene DL, Rockland KS. White Matter Neurons in Young Adult and Aged Rhesus Monkey. Front Neuroanat. 2016;10:15.
134. Mohan A, Thalamuthu A, Mather KA, Zhang Y, Catts VS, Weickert CS, et al. Differential expression of synaptic and interneuron genes in the aging human prefrontal cortex. Neurobiol Aging. 2018;70:194-202.
135. Farhy-Tselnicker I, van Casteren ACM, Lee A, Chang VT, Aricescu AR, Allen NJ. Astrocyte-Secreted Glypican 4 Regulates Release of Neuronal Pentraxin 1 from Axons to Induce Functional Synapse Formation. Neuron. 2017;96(2):428-45.e13.
136. Kucukdereli H, Allen NJ, Lee AT, Feng A, Ozlu MI, Conatser LM, et al. Control of excitatory CNS synaptogenesis by astrocyte-secreted proteins Hevin and SPARC. Proc Natl Acad Sci U S A. 2011;108(32):E440-9.

137. Rothstein JD, Dykes-Hoberg M, Pardo CA, Bristol LA, Jin L, Kuncl RW, et al. Knockout of glutamate transporters reveals a major role for astroglial transport in excitotoxicity and clearance of glutamate. Neuron. 1996;16(3):675-86.
138. Fabricius K, Jacobsen JS, Pakkenberg B. Effect of age on neocortical brain cells in 90+ year old human females--a cell counting study. Neurobiol Aging. 2013;34(1):91-9.
139. Walløe S, Pakkenberg B, Fabricius K. Stereological estimation of total cell numbers in the human cerebral and cerebellar cortex. Front Hum Neurosci. 2014;8:508.
140. Melo P, Magalhães A, Alves CJ, Tavares MA, de Sousa L, Summavielle T, et al. Methamphetamine mimics the neurochemical profile of aging in rats and impairs recognition memory. Neurotoxicology. 2012;33(3):491-9.
141. Vašák M, Meloni G. Mammalian Metallothionein-3: New Functional and Structural Insights. Int J Mol Sci. 2017;18(6).
142. Chung RS, Adlard PA, Dittmann J, Vickers JC, Chuah MI, West AK. Neuron-glia communication: metallothionein expression is specifically up-regulated by astrocytes in response to neuronal injury. J Neurochem. 2004;88(2):454-61.
143. West AK, Hidalgo J, Eddins D, Levin ED, Aschner M. Metallothionein in the central nervous system: Roles in protection, regeneration and cognition. Neurotoxicology. 2008;29(3):489-503.
144. Swindell WR. Metallothionein and the biology of aging. Ageing Res Rev. 2011;10(1):132-45.
145. Leung YK, Pankhurst M, Dunlop SA, Ray S, Dittmann J, Eaton ED, et al. Metallothionein induces a regenerative reactive astrocyte phenotype via JAK/STAT and RhoA signalling pathways. Exp Neurol. 2010;221(1):98-106.
146. Tanaka Y, Mizoguchi K. Influence of aging on chondroitin sulfate proteoglycan expression and neural stem/progenitor cells in rat brain and improving effects of a herbal medicine, yokukansan. Neuroscience. 2009;164(3):1224-34.
147. Fehon RG, McClatchey AI, Bretscher A. Organizing the cell cortex: the role of ERM proteins. Nat Rev Mol Cell Biol. 2010;11(4):276-87.
148. Lavialle M, Aumann G, Anlauf E, Pröls F, Arpin M, Derouiche A. Structural plasticity of perisynaptic astrocyte processes involves ezrin and metabotropic glutamate receptors. Proc Natl Acad Sci U S A. 2011;108(31):12915-9.
149. Freymuth PS, Fitzsimons HL. The ERM protein Moesin is essential for neuronal morphogenesis and long-term memory in Drosophila. Mol Brain. 2017;10(1):41.
150. Persson A, Lindberg OR, Kuhn HG. Radixin inhibition decreases adult neural progenitor cell migration and proliferation in vitro and in vivo. Front Cell Neurosci. 2013;7:161.
151. Moon Y, Kim JY, Kim WR, Kim HJ, Jang MJ, Nam Y, et al. Function of ezrin-radixin-moesin proteins in migration of subventricular zone-derived neuroblasts following traumatic brain injury. Stem Cells. 2013;31(8):1696-705.
152. Matsui T, Yonemura S, Tsukita S. Activation of ERM proteins in vivo by Rho involves phosphatidyl-inositol 4-phosphate 5-kinase and not ROCK kinases. Curr Biol. 1999;9(21):1259-62.
153. Shaw RJ, Henry M, Solomon F, Jacks T. RhoA-dependent phosphorylation and relocalization of ERM proteins into apical membrane/actin protrusions in fibroblasts. Mol Biol Cell. 1998;9(2):403-19.
154. Yonemura S, Matsui T, Tsukita S. Rho-dependent and -independent activation mechanisms of ezrin/radixin/moesin proteins: an essential role for polyphosphoinositides in vivo. J Cell Sci. 2002;115(Pt 12):2569-80.
155. Briscoe J, Thérond PP. The mechanisms of Hedgehog signalling and its roles in development and disease. Nat Rev Mol Cell Biol. 2013;14(7):416-29.
156. Farmer WT, Abrahamsson T, Chierzi S, Lui C, Zaelzer C, Jones EV, et al. Neurons diversify astrocytes in the adult brain through sonic hedgehog signaling. Science. 2016;351(6275):849-54.

157. Chechneva OV, Deng W. Empowering sonic hedgehog to rescue brain cells after ischemic stroke. Neural Regen Res. 2015;10(3):360-2.
158. Baruch K, Deczkowska A, David E, Castellano JM, Miller O, Kertser A, et al. Aging. Aging-induced type I interferon response at the choroid plexus negatively affects brain function. Science. 2014;346(6205):89-93.
159. Zhang G, Li J, Purkayastha S, Tang Y, Zhang H, Yin Y, et al. Hypothalamic programming of systemic ageing involving IKK-β, NF-κB and GnRH. Nature. 2013;497(7448):211-6.
160. Payán-Gómez, C.; Rodríguez, D.; Amador-Muñoz, D.; Ramírez-Clavijo, S. Integrative Analysis of Global Gene Expression Identifies Opposite Patterns of Reactive Astrogliosis in Aged Human Prefrontal Cortex. Brain Sci. 2018, 8, 227.
161. Krstic D, Madhusudan A, Doehner J, Vogel P, Notter T, Imhof C, et al. Systemic immune challenges trigger and drive Alzheimer-like neuropathology in mice. J Neuroinflammation. 2012;9:151.
162. Jongbloed F, de Bruin RW, Klaassen RA, Beekhof P, van Steeg H, Dor FJ, et al. Short-Term Preoperative Calorie and Protein Restriction Is Feasible in Healthy Kidney Donors and Morbidly Obese Patients Scheduled for Surgery. Nutrients. 2016;8(5).